

0142989
TECH LIBRARY KAFB, NM



RESEARCH MEMORANDUM

AN EMPIRICALLY DERIVED METHOD FOR CALCULATING PRESSURE
DISTRIBUTIONS OVER AIRFOILS AT SUPERCRITICAL MACH
NUMBERS AND MODERATE ANGLES OF ATTACK

By

Gerald E. Nitzberg and Loma E. Sluder

Ames Aeronautical Laboratory
Moffett Field, Calif.

CLASSIFIED DOCUMENT

This document contains classified information affecting the National Defense of the United States within the meaning of the Espionage Act, USC 50:31 and 32. Its transmission or the revelation of its contents in any manner to an unauthorized person is prohibited by law. Information so classified may be imparted only to persons in the military and naval services of the United States, appropriate civilian officers and employees of the Federal Government who have a legitimate interest therein, and to United States citizens of known loyalty and discretion who of necessity must be informed thereof.

AFMDC
TECHNICAL LIBRARY
AFL 2811

NATIONAL ADVISORY COMMITTEE FOR AERONAUTICS

WASHINGTON

April 1, 1947


CONFIDENTIAL

719.98/13

A 7 B 07

6265

Patented 5 May 1949
authorized by notice of declassification of publications No. 1, March 1949

EAT
TECH LIBRARY KAFB, NM

0142989

NACA RM. NO. A7B07

CONFIDENTIAL

NATIONAL ADVISORY COMMITTEE FOR AERONAUTICS

RESEARCH MEMORANDUM

AN EMPIRICALLY DERIVED METHOD FOR CALCULATING PRESSURE
DISTRIBUTIONS OVER AIRFOILS AT SUPERCRITICAL MACH
NUMBERS AND MODERATE ANGLES OF ATTACK

By Gerald E. Nitzberg and Loma E. Sluder

SUMMARY

On the basis of an analysis of experimental airfoil data a procedure is developed for calculating pressure distributions over airfoils at supercritical Mach numbers. A number of factors limit application of the method to moderate angles of attack. Only the forward portion of the airfoil, where interaction between local boundary-layer thickness and local-pressure distribution is negligible, is considered in detail. Use of the method developed merely requires a knowledge of the low-speed or potential theory, pressure distribution, and the shape of the airfoil. Calculated and experimentally measured high-speed pressure distributions are compared for a wide variety of airfoils at different angles of attack and Mach numbers.

INTRODUCTION

Air, when flowing past moderately thick airfoil sections at seven- or eight-tenths the velocity of sound, attains local velocities in excess of sonic. Analysis of such mixed subsonic and supersonic types of flow presents difficulties which are greater than those of either purely subsonic or supersonic flow.

A general compressibility correction for pressure coefficients has been derived by Kármán and Tsien (reference 1) which, when applied to potential theory pressure distributions, gives the distribution over an airfoil in any desired wholly subsonic flow. In the regime of purely supersonic flow, Prandtl and Meyer (reference 2) derived a theory of the pressure distribution over a curved surface by considering the effects on an initially semi-infinite uniform flow at sonic velocity when it is deflected around a corner. It was found that the local supersonic Mach numbers attained by the stream are a function only of the total angle through which the stream is turned. This theory can be used to obtain the pressure distributions over airfoils at supersonic Mach numbers. The supersonic flow region in the vicinity of airfoils at high subsonic free-stream Mach numbers is limited in extent so that the Prandtl-Meyer theory cannot be applied directly. As a result of mathematical difficulties, a

readily applicable solution of the problem of supersonic flow of limited extent has not been obtained as yet, but the importance of the problem makes it expedient to resort to an empirical analysis.

Pressure distributions over a number of airfoils at high Mach numbers have recently been obtained in the Ames 1- by 3-1/2-foot high-speed wind tunnel. The airfoils are of the conventional sections NACA 0015, 23015, 4415 and 4412, and the low-drag sections NACA 652-215 ($a = 0.5$) and 66,2-215 ($a = 0.6$). These pressure distributions were obtained at Reynolds numbers of approximately 2,000,000 and are considered to be accurate representations of free-air results up to Mach numbers of 0.810 for moderate angles of attack. The effects of Reynolds number variation on high-speed pressure distributions are not known. Therefore, it is not possible to estimate what restrictions are imposed on the generality of an analysis based on these pressure measurements as a result of the moderate test Reynolds number.

Experimental section drag coefficients were obtained by wake surveys simultaneously with the pressure distributions. At moderate angles of attack, the drag coefficients show no appreciable variation with Mach number until the local velocity of sound is exceeded at some point on the airfoil surface. The free-stream Mach number at which local sonic velocity first occurs is the critical Mach number. Above

the critical Mach number, there is a more or less marked increase in the airfoil drag coefficient. Since a drag increase is indicative of a thickening boundary layer, it is anticipated that there are considerable boundary-layer effects at supercritical speeds. It would thus appear possible to start an analysis of the experimental pressure distributions by separating the viscosity and compressibility effects. In reference 3, it is shown that the differences between airfoil section characteristics in potential flow and in real viscous fluids can be accurately treated by taking account of the boundary layer. These differences were found to be chiefly embodied in effective changes in the airfoil shape and angle of attack. It thus might be hoped that the compressible supercritical counterpart of potential theory could be obtained by correcting the experimental pressure distributions for the boundary-layer viscosity effects. Reference 4 has treated the growth and stability of the laminar boundary layer at large Mach numbers; but a survey of the literature reveals that boundary-layer changes through and behind shock waves have not yet been successfully analyzed. Moreover, there are a number of indications of a strong interaction between the shock wave and boundary layer which eliminates the possibility of separating viscosity and compressibility effects in the vicinity of the shock wave. In spite of this limitation, it still seems feasible to

separate gross viscosity effects, such as effective angle-of-attack changes, from the compressibility effects.

The initial step in the procedure used in the present report was the determination of all the known airfoil parameters, that is, the directly determinable properties of the airfoil and the flow field. These parameters were correlated with that property of the pressure distribution under consideration to find the ones which seem relevant. The result of such a procedure is not rigorously correct because it is based only on combinations of those parameters which are available. In other words, if some other parameter could be obtained, a combination of parameters might be found which would give equal or better correlation with the experimental measurements. Thus, the acceptance of the results of this report is dependent upon the rationality of the analysis based upon those parameters which are taken to be of prime importance.

ANALYSIS

At supercritical Mach numbers, where the flow in the vicinity of an airfoil is both subsonic and supersonic, it is to be expected that the relative importance of local airfoil-shape parameters will be different for these two types of flow. Therefore, these two regimes will be considered separately.

Forward Subsonic Region

A procedure for handling the forward subsonic region of the pressure distribution is suggested by analogy with the low-speed theory of viscosity effects on airfoil characteristics. This theory shows that the presence of a thick boundary layer results in an effective change in the angle of attack and camber line. The relatively large drag coefficients at supercritical Mach numbers are indicative of thick boundary layers. Therefore, it is to be expected that there is an effective angle-of-attack change at supercritical Mach numbers.

A study of experimental data at supercritical Mach numbers reveals that, for the airfoils tested, which were of 12- and 15-percent thickness, the subsonic region is of very limited chordwise extent on at least one surface at most angles of attack. In fact, at large Mach numbers the subsonic portion of the pressure distribution over both airfoil surfaces is greater than a few percent of a chord length at only moderate angles of attack, that is, angles from 0° to 4° . So in order to handle the subsonic regime, the analysis will have to be limited to such moderate angles of attack. The primary importance of studying the subsonic portion of the pressure distribution is as a means for predicting the chordwise location of the point at which sonic velocity is attained. In order to obtain a procedure which can be applied to an

arbitrary airfoil section, it is necessary to relate supercritical pressure distributions to low-speed pressure distributions. To do this, it would seem possible to apply the Kármán-Tsien theory to low-speed pressure distributions at angles of attack corrected for the high-speed boundary-layer effects. However, the experimental observations which are to be discussed directly indicate that in the immediate vicinity of the airfoil stagnation point the variation of pressure coefficient with Mach number does not seem to follow the Kármán-Tsien theory. An examination of subcritical pressure distributions, at angles of attack for which the drag coefficient remained constant with the increasing Mach number, revealed that at $2\frac{1}{2}$ - and 5-percent-chord stations the experimental pressure-coefficient variation with Mach number was less than that predicted by the Kármán-Tsien theory, while the variation aft of the 10-percent-chord station was in good agreement with the theory. At supercritical Mach numbers there are other factors besides compressibility which affect the variation with Mach number of pressure coefficients in the forward subsonic portion of the airfoil so that it was not feasible to investigate the observed deviation from theory in detail. Lacking a more appropriate compressibility correction, the present analysis will apply the Kármán-Tsien theory even near the airfoil leading edge.

In low-speed viscous theory, an effective angle-of-attack change is considered to occur when the presence of a boundary layer alters the flow past an airfoil in a manner which is similar to that which would arise from a shift of the airfoil trailing edge from its actual physical position to an effective position at the center of the total trailing-edge boundary layer. Thus, to find the effective angle-of-attack change, it is only necessary to know the trailing-edge boundary-layer thickness for each surface of the airfoil. At low speeds the drag coefficient is a known function of boundary-layer thickness and pressure coefficient at the trailing edge. However, this functional relation is not known for supercritical speeds. Moreover, at supercritical Mach numbers, drag has two components - losses through the shock wave and within the boundary layer. It is not to be expected that the shock-wave wake would operate like the boundary layer, in changing the effective angle of attack. Therefore, the trailing-edge boundary-layer thickness cannot be directly determined at supercritical Mach numbers from the known pressure distribution and drag coefficient.

That portion of the experimental pressure distributions ahead of the sonic point was reduced to low speeds by using the Kármán-Tsien theory. When these adjusted pressure distributions were compared with low-speed pressure distributions, it was found that the upper and lower surfaces of an

airfoil appeared to be at different angles of attack. The adjusted pressure distributions over single surfaces did not conform exactly to the low-speed distribution for any angle of attack; however, over the forward subsonic portion of each pressure distribution, the maximum scatter corresponded to a spread of a few tenths of a degree. This similarity indicates that, as a first approximation, the total boundary-layer effect can be treated as an angle-of-attack change. A precise evaluation of boundary-layer effects would require separating the angle-of-attack effect and the shape change. There is no available method for calculating boundary-layer changes in the vicinity of a shock wave so the present analysis is limited to the previously mentioned first approximation.

The effective angle of attack for each airfoil surface was calculated from the experimental pressure distributions for which only one surface had a region of supersonic flow. For the moderate angles of attack considered, the supersonic region always occurred on the upper surface of the airfoil. The values of the effective angle-of-attack change, occasioned by the presence of a shock on the upper surface $\Delta\alpha$ (U.S.S.) were plotted for each surface as a function of the increment of the free-stream Mach number above the critical Mach number $M-M_{cr}$. Values were plotted for the upper surface in figure 1 and those for the lower surface in figure 2. In these

figures it is seen that for the wide variety of airfoil shapes and differences in free-stream Mach number and geometric angles of attack, the maximum dispersion of the points for any value of $M - M_{Cr}$ is only about 1° . Therefore, a curve faired through the mean values of the experimental points can be used to predict the effective angle-of-attack change for a given value of $M - M_{Cr}$ to within about $1/2^\circ$. Although this approximation is adequate for predicting the sonic-point location, an attempt was made to determine whether this dispersion was a function of some other parameter. A parameter which seemed to be of considerable importance was $dM_{Cr}/d\alpha$. It was noticed that the majority of the cases for which $\Delta\alpha(U.S.S.)$ values were low corresponded to configurations having values of $dM_{Cr}/d\alpha$ greater than 0.025. Further evidence of the importance of this parameter is presented in figure 3 where the increment of drag coefficient above the low-speed drag coefficient $C_D - C_{D_{L.S.}}$ is plotted as a function of $M - M_{Cr}$, for the configurations considered in figures 1 and 2. Figure 3 shows that, for all but one configuration, a curve can be drawn separating the points having large and small values of $dM_{Cr}/d\alpha$. A method, based on this parameter, has been developed for predicting the effective angle of attack with greater accuracy; however, the theoretical critical Mach numbers are not in sufficiently close agreement with experimentally measured values to justify the use of this

more involved method.

The critical Mach number of an airfoil at a given geometric angle of attack can be found by applying the Kármán-Tsien compressibility correction to the airfoil peak-pressure coefficient obtained from potential theory. This procedure has been used in reference 5. It is found that the variation of critical Mach number of each surface of an airfoil with angle of attack is different for airfoils of different shapes, and, even for a given airfoil, there are two markedly different angle-of-attack regimes for each surface in which this difference in variation is apparent. One regime, usually positive angles of attack for lower surfaces and negative angles for upper surfaces, includes angles for which the peak-pressure coefficient is determined chiefly by the airfoil-thickness distribution and camber, and consequently there is little change of critical Mach number with angle of attack. In the other regime, the maximum-pressure peak occurs near the airfoil nose as a result of the additional lift distribution, that is, the increased circulation resulting from pitching the airfoil. There is considerable uncertainty as to the accuracy of the calculations of critical Mach numbers at these angles because of the previously discussed deviation of the flow near the stagnation point from the Kármán-Tsien theory. In this regime, uncertainty also exists for critical Mach numbers determined from high-speed experimental pressure distributions unless a number of pressure orifices have been

placed along the forward 5 percent of the airfoil chord. This limitation places serious restriction on a significant source of information regarding the high-speed characteristics of airfoils.

The experimental and theoretical critical Mach number curves for both surfaces of the airfoils considered are shown as a function of angle of attack in figure 4. As will be discussed directly, in the present method of analysis, a correction to the theoretical curves is required.

When only one surface is at a supercritical Mach number there is an effective angle-of-attack change of the other surface which results in a change in the pressure distribution and thus in the critical Mach number of the latter surface. Therefore, if the critical Mach number curves are obtained theoretically, it is necessary to adjust the calculated values for the surface with the higher critical Mach number to account for the effective angle-of-attack change due to the shock wave on the other surface of the airfoil. Curves thus derived are in reasonable agreement with experimental measurements.

As was indicated previously, when the free-stream Mach number M is above the critical Mach number of only one surface of an airfoil, the following procedure can be used to calculate the subsonic portion of the pressure distribution over the airfoil. The critical Mach number M_{cr} , for the moderate geometrical angle of attack under consideration, is computed from the low-speed pressure

distribution by means of the Kármán-Tsien theory. Curves of the Kármán-Tsien compressibility correction are given in figure 5. Then having the value of $M - M_{cr}$, the curve of figure 1 is used to estimate the effective angle of attack for the surface of the airfoil over which the local region of supersonic flow occurs. The subsonic portion of the pressure distribution over this surface of the airfoil at the free-stream Mach number under consideration is obtained by applying the Kármán-Tsien compressibility correction to the low-speed pressure distribution corresponding to the effective angle of attack. The flow over the other airfoil surface is entirely subsonic so that the pressure distribution can be estimated directly. The effective angle of attack of this surface is obtained from the curve of figure 2 by using the same value of $M - M_{cr}$ as used in figure 1.

The previously mentioned procedure can be generalized to apply to the case of airfoils at Mach numbers above the critical speed of both surfaces if the assumption is made that the effects of the supersonic region on each surface are additive. In this case, it is necessary to obtain the critical Mach number for each surface of the airfoil. Then using the upper-surface Mach number increment above its critical $(M - M_{cr_U})$ the effective angle-of-attack changes, due to the upper-surface supersonic region of flow, for the upper surface $\Delta\alpha(U.S.S.)_U$ and lower surface $\Delta\alpha(U.S.S.)_L$

of the airfoil are obtained from figures 1 and 2, respectively. Similarly, for the lower-surface increment above its critical ($M - M_{crL}$) the effective angle-of-attack changes, due to the lower-surface supersonic region of flow, for the lower surface $\Delta\alpha(L.S.S.)_L$ and upper surface $\Delta\alpha(L.S.S.)_U$ are obtained from figures 1 and 2, respectively. The total effective angle-of-attack change is then $\Delta\alpha(U.S.S.)_U - \Delta\alpha(L.S.S.)_U$ for the upper surface, and $\Delta\alpha(U.S.S.)_L - \Delta\alpha(L.S.S.)_L$ for the lower surface.

The limited experimental data used to derive the aforementioned general procedure make it of dubious accuracy at Mach numbers above $M - M_{cr}$ of 0.20. Below this limit the maximum difference between the calculated angle of attack of a surface, predicted by this procedure, and that obtained from the experimental pressure distribution was about $1/2^\circ$.

The preceding method can be used to predict the chordwise location of the point at which sonic velocity is first attained. The pressure coefficient corresponding to sonic velocity at a given free-stream Mach number may be obtained from figure 5. The movement of the sonic point with Mach number has been predicted using this procedure for the airfoils for which experimental pressure distributions are available. The method is applicable for the normal operating range of high-speed airplanes, that is, angles of attack from 0° to 4° and Mach number increments less than 0.20 above the critical. In this range the difference between the calculated value and

the experimentally measured sonic point was less than a few percent of a chord length.

Region of Increasing Supersonic Local Mach Numbers

The Kármán-Tsien compressibility correction is strictly limited to subsonic regions of the pressure distribution. The only available procedure for supersonic flows is that of Prandtl and Meyer, which presents the local Mach number as a function of the difference between the local surface slope and the slope at the sonic point. The local Mach number is uniquely related to the pressure coefficient for a given free-stream Mach number. This relationship is shown in figure 6. To study the supersonic portion of the airfoil pressure distribution at moderate angles of attack, local Mach number was plotted as a function of the change in slope of the surface from that at the sonic point. It was found that the variation was similar to the Prandtl-Meyer theory but different configurations achieved varying percentages of the theoretical local Mach number rise above unity corresponding to a given slope change. The Prandtl-Meyer theoretical increase in local Mach number for expansive deflection of the stream from its direction at sonic velocity and several percentages of this theoretical variation are presented in figure 7. For a given airfoil, angle of attack, and Mach number, the local Mach numbers

attained conformed closely to a unique percentage of the Prandtl-Meyer theoretical results. This failure to obtain the full theoretical rise of local Mach number seems reasonable because the Prandtl-Meyer theory is based on the assumption of a semi-infinite uniform sonic flow deflected around a curved surface; whereas, airfoils at supercritical Mach numbers have a supersonic region of very limited extent. The extent and uniformity of this supersonic region depends on such factors as the free-stream Mach number, the critical Mach number, and the chordwise location of the sonic point.

One variable chosen was "Percent of Prandtl-Meyer" and this was correlated with all known airfoil parameters which seemed relevant. These parameters included $M - M_{cr}$, the surface curvature at the sonic point and also at the point at which a local Mach number of 1.2 occurs, the slope of the airfoil surface at the sonic point relative to the free-stream direction and also relative to the airfoil chord line, the chordwise location of sonic velocity and local Mach number of 1.2, and others. It was found that the two parameters which gave the best correlation with percent of Prandtl-Meyer were $M - M_{cr}$ and the slope of the surface at the sonic point relative to the airfoil chord line. Measuring slope relative to the airfoil chord line seems strange at first consideration but, since for the configurations considered, the stagnation point very nearly coincides with the forward end of the chord

line, there seems to be some physical basis for using the airfoil chord as a reference line. The data which were analyzed included cases for which the included angle θ_s between a tangent to the surface at the sonic point and the airfoil chord line varied from 5° to 30° . Within this range it was observed that for equal values of $M - M_{cr}$ the percent of Prandtl-Meyer attained decreased with increasing θ_s . It should be mentioned that increasing values of θ_s correspond to movement of the sonic point toward the airfoil leading edge. The other variation noted was that increasing $M - M_{cr}$ for constant values of θ_s resulted in increasing the percent of Prandtl-Meyer which was attained. Curves based on the experimental data are presented in figure 8. The maximum difference between experimental values and these curves corresponded to a 5-percent shift in percent of Prandtl-Meyer.

Once the slope distribution over the airfoil and the sonic-point location are determined, the supersonic portion of the pressure distribution can be calculated as follows: The percentage of the Prandtl-Meyer theoretical curve which should be used is determined from figure 8. The local Mach numbers reached at any chordwise station are obtained from the particular percentage curves shown in figure 7. When the curves of figure 6 are used, these local Mach numbers can be converted directly to pressure coefficients S .

Of course, this analysis is based on the use of percent of Prandtl-Meyer as a parameter and thus can only be considered to be empirically derived.

Termination of the Supersonic Regime

There is nothing in the foregoing analysis to give any clue as to the chordwise point of termination of the supersonic region. It was believed that there was a very direct relation between the stability of the boundary layer and the location of the shock wave. To check this hypothesis, pressure distributions over a carefully cleaned NACA 4412 airfoil were obtained at a moderate angle and various Mach numbers in the Ames 1- by 3-1/2-foot high-speed wind tunnel. Then grains of carborundum were attached between the 5- and 10-percent chordwise stations on the airfoil, and pressure distributions at the same angle and Mach numbers were obtained. The pressure recovery, corresponding to the shock wave, was much more abrupt but only slightly further forward for the roughened airfoil than for the smooth airfoil. The pressure distribution in the region of increasing supersonic local Mach numbers was the same for the two airfoil surface conditions. It is not feasible to make a quantitative analysis of this phenomenon since there are no available theories of laminar separation, transition from laminar to turbulent boundary-layer flow, or turbulent separation, in supersonic flows.

Even more important, there are no quantitative results for the interaction between such boundary-layer changes and shock waves. For the pressure distributions available on airfoils of 12- and 15-percent thickness, for moderate angles of attack at Mach numbers between 0.05 and 0.20 above the critical, it was noticed that the point at which the local supersonic Mach numbers ceased to increase corresponded roughly to that point, on the surface under consideration, at which the surface was tangent to the free-stream direction. It is not immediately apparent why this geometrically determined parameter should so influence the flow past the airfoil.

There is usually no precise location of a shock wave discernible from the pressure distributions. Instead of an abrupt discontinuity there is a gradual pressure recovery. These pressure distributions were obtained by means of a liquid manometer so that they may represent a time average pressure distribution of an unsteady flow condition. Alternatively, the gradual pressure recovery observed may be a result of a thick boundary layer. This boundary layer may soften the shock as discussed in reference 6. Also, the abrupt pressure change might be masked by the boundary-layer thickness, but this seems unlikely since, as has been previously mentioned, an abrupt pressure recovery was observed on the roughened NACA 4412 airfoil. It is expected that, since airfoil surface roughness causes marked changes

in the nature of the pressure recovery which accompanies transition from supersonic to subsonic flow, Reynolds number might have important effects on the shock wave. In all the configurations analyzed it was found that the position on the airfoil surface at which the local Mach number had dropped to unity could be estimated by applying the Kármán-Tsien compressibility correction to the potential theory pressure distribution. It was therefore decided to terminate the supersonic portion of the pressure-distribution calculations at the chordwise station for which a local Mach number of unity is predicted.

The experimental pressure distributions indicate a more or less gradual pressure recovery over the region from the chordwise station at which the surface is tangent to the free-stream direction to that station at which a local Mach number of unity occurs. When the local pressure coefficients for these two stations are connected by a straight line, it is noticed that the local portion of the experimental pressure distribution lies near this line or between this line and the calculated supersonic pressure distribution. The presence of this region of decreasing supersonic local Mach numbers is believed to be due to interaction between the local boundary layer and the shock wave.

Estimation of Pressure Distribution Aft
of Supersonic Region

Over the rear portion of an airfoil, behind a shock wave, the boundary layer is probably quite thick. It is to be expected that a thick boundary layer could have considerable effect on the local pressure distribution. However, there are no available methods for calculating the boundary-layer thickness behind a shock wave. Therefore, in the present report the subsonic portion of the pressure distribution over the rear of the airfoil will be approximated by applying the Kármán-Tsien compressibility correction to the local potential theory pressure distribution.

DISCUSSION

The primary concern of the preceding analysis is the prediction of supercritical pressure distributions over the forward portion of airfoils. The detailed analysis is restricted to this portion of the airfoil where local boundary-layer thickness does not markedly alter the local pressure distribution. Before comparing calculated and experimental pressure distributions, some of the general problems which arise will be reviewed.

In comparing the low-speed or potential theory pressure distribution to those at moderately high Mach numbers, it is found, as would be expected, that the Kármán-Tsien theory

is inaccurate near the nose of the airfoil. There is no available procedure for treating this region. Therefore, in the preceding analysis the assumption is made that the Kármán-Tsien theory provides an adequate approximation for pressure coefficients at points close to the airfoil leading edge. However, the errors introduced by the assumption are of secondary importance at moderate angles of attack. An investigation is needed to determine how pressure coefficients change with Mach number at the nose of the airfoil.

The airfoil-surface slope changes rapidly in the vicinity of the airfoil nose. When the sonic point occurs in this region, there may be considerable error in the determination of the surface slope at the sonic point. Fortunately, the present method compensates for errors in the sonic-point slope. For example, if too large a sonic-point slope is read for a given value of $M - M_{cr}$, too small a percentage of Prandtl-Meyer theory would be obtained from figure 8. Since local Mach number attained varies with both the surface-slope change from the sonic point and the percent of Prandtl-Meyer, and an excessive value of one results in a diminished value of the other, it is seen that these two effects tend to counterbalance each other, except in the immediate vicinity of the sonic point.

The present method can be expected to give rather good accuracy in determining the peak-pressure coefficients and the maximum load obtained on the forward portion of the airfoil.

However, a factor which may contribute to differences between calculations and experimental measurements for airplane wings is the fact that the supersonic portion of the pressure distribution depends upon the airfoil-surface slope. As a result of practical construction difficulties, there are discrepancies in the actual wing profile which give rise to uncertainties regarding the surface slope.

Application of Method

In order to evaluate the utility and limitations of the procedure which has been developed, this method has been used to calculate the various configurations for which experimental results are available. As has been pointed out, the development of the method limits its application to moderate angles of attack and to Mach numbers less than 0.20 above the critical Mach number. For angles of 0° , 2° , and 4° , two supercritical Mach numbers have been considered for each airfoil. The calculated characteristics of all the configurations are tabulated in table I.

For incompressible potential theory, it is usual to obtain the velocity distribution rather than the pressure distribution. The additional lift due to pitching the airfoil is directly additive to the basic velocity distribution so that the velocity distribution is particularly convenient for treating cases for which several angles of attack are considered. Since velocity distribution is so easily modified, it was decided to use the

pressure coefficient S , which, at low speeds, is the square of the ratio of the local velocity and the free-stream velocity. In figure 5 the Kármán-Tsien theoretical variation of pressure coefficient S with Mach number is presented. The supersonic theory of Prandtl-Meyer is in terms of the local Mach number. Figure 6 gives the pressure coefficient S corresponding to a local Mach number as a function of free-stream Mach number.

As has been previously mentioned, it was noticed that the termination of the supersonic regime of rising pressure coefficients occurs approximately at the point where the airfoil surface is parallel to the effective free-stream direction. In the calculated pressure distributions this point is connected with the rearward sonic point by a straight line.

As an example of pressure-distribution variation with Mach number for a fixed geometric angle of attack the NACA 652-215 airfoil at 2° is considered. Figure 9 shows a comparison of the calculated pressure-distribution curves and the experimental points at Mach numbers of 0.700, 0.725, 0.750, 0.775, 0.800, and 0.825. The present method has a lower limit of applicability at $M - M_{cr}$ of 0.05 because of the very limited supersonic region for such slightly supercritical Mach numbers. An approximate value of the pressure distribution in this regime is obtained by applying the Kármán-Tsien compressibility correction for the entire pressure distribution. At Mach numbers of 0.775 and 0.800

the lower surface is only slightly supercritical and applying the Kármán-Tsien theory gives inaccurate values for the peak-pressure coefficients. Both surfaces are well above their respective critical Mach numbers at 0.825 so the present method can be applied to both surfaces. The large drag coefficient at this Mach number indicates a thick boundary layer at the rear of the airfoil which may be the cause of poor accuracy of Kármán-Tsien theory in this region. Throughout the Mach number range the calculations give a good prediction of the peak-pressure coefficients and of the load over the forward 40 percent of the chord length.

Now consider the same airfoil at different angles of attack. At 0° and 4° , the marked difference in the type of loading for the low and high supercritical Mach numbers is correctly represented by the calculations.

In figure 10, it is seen that the method works well for the NACA 66,2-215 airfoil at 0° and 2° . As a result of the small leading-edge radius of this airfoil the upper-surface critical speed at 4° is determined by a pressure peak near the nose; therefore, the critical speed cannot be determined accurately. However, this is a borderline case in that the forward pressure peak is not very sharp, so the critical Mach number was based on the farthest forward experimental pressure point. The calculated pressure distributions based on this critical Mach number are presented to show the magnitude of

the error that can be expected for such borderline cases.

For the NACA 4412 airfoil at 0° , 2° , and 4° the change in type of loading with Mach number is accurately predicted.

There was some inaccuracy in the construction of the NACA 0015 airfoil as can be seen in figure 12 from the difference between the experimental pressure distribution for the two surfaces at 0° . At 2° for $M = 0.725$ and at 4° for both Mach numbers shown, the upper-surface shock is very far forward. The start of the marked pressure recovery is still at the point at which the airfoil surface is tangent to the free-stream direction.

The comparisons of experiment and theory for the NACA 23015 are presented in figure 13. At 0° , 2° , and 4° the shock occurs far forward, but the load distribution and pressure peaks are well represented.

It is interesting to notice the similarity between the results for the NACA 4415 airfoil in figure 14 and the NACA 4412 in figure 11. The values of $M + M_{cr}$ used in figure 14 were chosen to be as close as possible to those for the corresponding angles of attack in figure 11. The agreement between calculation and experiment in the vicinity of the nose is not as good for the NACA 4415 airfoil as for the NACA 4412 airfoil because of the difficulty arising as a result of the large leading-edge radius of the former airfoil.

CONCLUDING REMARKS

The procedure which has been developed provides a satisfactory prediction of the supersonic portion of the supercritical pressure distributions for airfoils at moderate angles of attack. The parameters on which the procedure is based were limited to those which were determinable from potential theory pressure distributions and the geometric properties of the airfoils. This method, therefore, cannot be considered definitive. It is primarily a useful means for predicting maximum loads and peak-pressure coefficients. Further experimental investigation of conditions in the vicinity of the airfoil nose at high Mach numbers should permit an extension of the method to a wider angle-of-attack range.

Ames Aeronautical Laboratory,
National Advisory Committee for Aeronautics,
Moffett Field, Calif.

Gerald E. Nitzberg
Gerald E. Nitzberg,
Aeronautical Engineer.

Loma E. Sluder,
Physicist.

Approved:

Donald H. Wood
eed
Donald H. Wood,
Aeronautical Engineer.

REFERENCES

1. von Kármán, Th.: Compressibility Effects in Aerodynamics. Jour. Aero. Sci., vol. 8, no. 9, July 1941, pp.337-356.
2. Taylor, G. I., and Maccoll, J. W.: Two-Dimensional Flow at Supersonic Speeds. Vol. III, div. H, ch. IV of Aerodynamic Theory, W. F. Durand, ed., Julius Springer (Berlin), 1935.
3. Nitzberg, Gerald E.: The Theoretical Calculation of Airfoil Section Coefficients at Large Reynolds Numbers. NACA ACR No. 4112, 1944.
4. Allen, H. Julian, and Nitzberg, Gerald E.: The Effect of Compressibility on the Growth of the Laminar Boundary Layer on Low-Drag Wings and Bodies. NACA ACR, Jan. 1943.
5. Heaslet, Max. A.: Critical Mach Numbers of Various Airfoil Sections. NACA ACR No. 4618, 1944.
6. Donaldson, Coleman duP.: Effects of Interaction Between Normal Shock and Boundary Layer. NACA CB No. 4427, 1944.

TABLE I.- SUPERCRITICAL-PRESSURE-DISTRIBUTION PARAMETERS

Airfoil section	α (deg)	M	M_{cr}		M - M_{cr}		$\Delta\sigma$ (U.S.S.)		$\Delta\alpha$ (L.S.S.)		$\Delta\alpha_{total}$		θ_{sonic}		Percent P - M			
			Upper surface	Lower surface	Upper surface	Lower surface	Upper surface	Lower surface	Upper surface	Lower surface	Upper surface	Lower surface	Upper surface	Lower surface	Upper surface	Lower surface		
65 ₂ -215	2	0.700	0.650	0.760	0.050	---	0.7	0.1	---	---	0.7	0.1	11.9	---	35	---		
		.725	.650	.760	.075	---	1.2	.3	---	---	1.2	.3	15.0	---	37	---		
		.750	.650	.760	.100	---	1.7	.6	---	---	1.7	.6	15.5	---	40	---		
		.775	.650	.760	.125	0.015	2.3	.9	0	.2	2.3	.7	14.5	---	44	---		
		.800	.650	.760	.150	.040	2.9	1.3	.1	.6	2.8	.7	13.0	---	48	---		
		.825	.650	.760	.175	.065	3.5	1.9	.2	1.0	3.3	.9	13.5	5.5	51	42		
	0	.750	.670	.750	.080	---	1.3	.3	---	---	1.3	.3	8.5	---	43	---		
		.800	.670	.750	.130	.050	2.4	1.0	.1	.7	2.3	.3	9.0	13.1	51	35		
		4	.725	.620	.775	.105	---	1.8	.6	---	---	1.8	.6	22.5	---	36	---	
			.800	.620	.775	.180	.025	3.6	2.0	.1	.3	3.5	1.7	18.5	---	46	---	
			66 ₂ -215	0	.750	.690	.760	.060	---	.9	.2	---	.9	.2	7.0	---	40	---
				.800	.690	.760	.110	.040	1.9	.7	.1	.6	1.8	.1	8.6	---	48	---
2	.750	.670	.770	.080	---	1.3	.3	---	---	1.3	.3	15.5	---	38	---			
	.800	.670	.770	.130	.030	2.4	1.0	.1	.4	2.3	.6	15.4	---	43	---			
	4	.725	.620	.770	.105	---	1.8	.6	---	---	1.8	.6	28.0	---	34	---		
		.800	.620	.770	.180	.030	3.6	2.0	.1	.4	3.5	1.6	20.0	---	45	---		
4412	0	.760	.635	.725	.125	.035	2.3	.9	.1	.5	2.2	.4	16.0	---	43	---		
	2	.810	.635	.725	.175	.080	3.5	1.9	.3	1.3	3.2	.6	15.0	36.0	49	31		
		.700	.595	.775	.105	---	1.8	.6	---	---	1.8	.6	22.0	---	37	---		
	4	.790	.595	.775	.195	.015	4.0	2.5	0	.2	4.0	2.3	18.0	---	48	---		
		.650	.560	.810	.090	---	1.5	.4	---	---	1.5	.4	34.0	---	32	---		
	0015	0	.775	.700	.700	.075	.075	1.2	.3	.3	1.2	.9	15.0	15.0	37	37		
2		.800	.700	.700	.100	.100	1.7	.6	.6	1.7	1.1	-1.1	18.4	18.4	38	38		
		.725	.650	.750	.075	---	1.2	.3	---	---	1.2	.3	22.0	---	34	---		
4		.800	.650	.750	.150	.050	2.9	1.3	.1	.7	2.8	.6	18.4	14.5	43	34		
	.675	.570	.770	.150	---	1.8	.6	---	---	1.8	.6	39.0	---	31	---			
23015	0	.750	.570	.770	.180	---	3.6	2.0	---	---	3.6	2.0	35.0	---	35	---		
	2	.725	.635	.740	.090	---	1.5	.4	---	---	1.5	.4	21.5	---	35	---		
		.800	.635	.740	.165	.060	3.2	1.6	.2	.9	3.0	.7	23.0	8.8	42	39		
	4	.675	.580	.765	.095	---	1.6	.5	---	---	1.6	.5	28.5	---	33	---		
		.750	.580	.765	.170	---	3.4	1.8	---	---	3.4	1.8	28.5	---	39	---		
	4415	0	.725	.535	.775	.115	---	2.0	.8	---	---	2.0	.8	32.0	---	33	---	
2		.730	.625	.705	.105	.025	1.8	.6	.1	.3	1.7	.3	19.0	---	38	---		
		.810	.625	.705	.185	.105	3.7	2.2	.6	1.8	3.1	.4	16.0	29.0	49	34		
4		.680	.590	.745	.090	---	1.5	.4	---	---	1.5	.4	23.0	---	35	---		
		.790	.590	.745	.200	.045	4.1	2.6	.1	.6	4.0	2.0	20.3	---	47	---		
23015		0	.650	.555	.780	.095	---	1.6	.5	---	---	1.6	.5	27.0	---	34	---	
	.735	.555	.780	.180	---	3.6	2.0	---	---	3.6	2.0	25.0	---	41	---			

CONFIDENTIAL

NAACA RM No. A7E07

CONFIDENTIAL

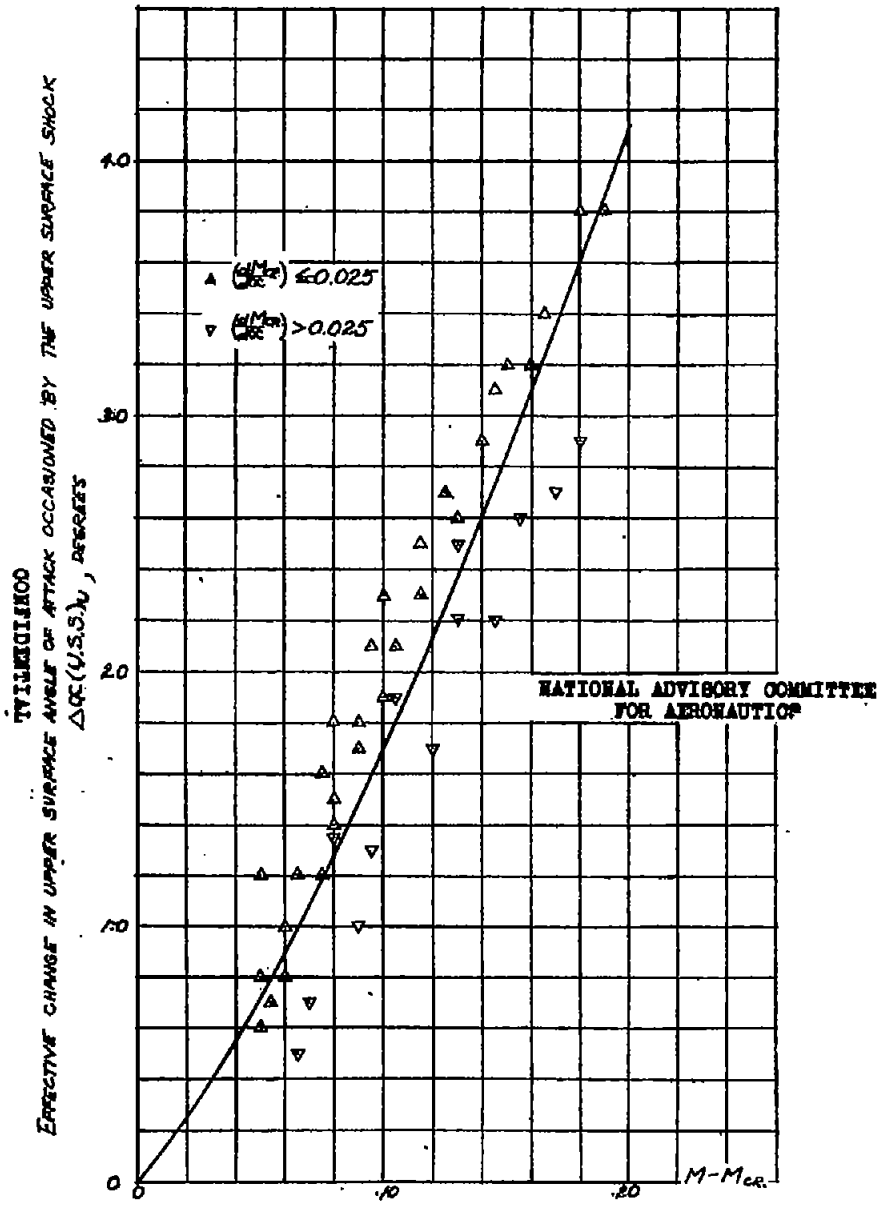


FIGURE 1.- EFFECTIVE CHANGE IN UPPER SURFACE ANGLE OF ATTACK WITH INCREMENT OF MACH NUMBER ABOVE THE CRITICAL.

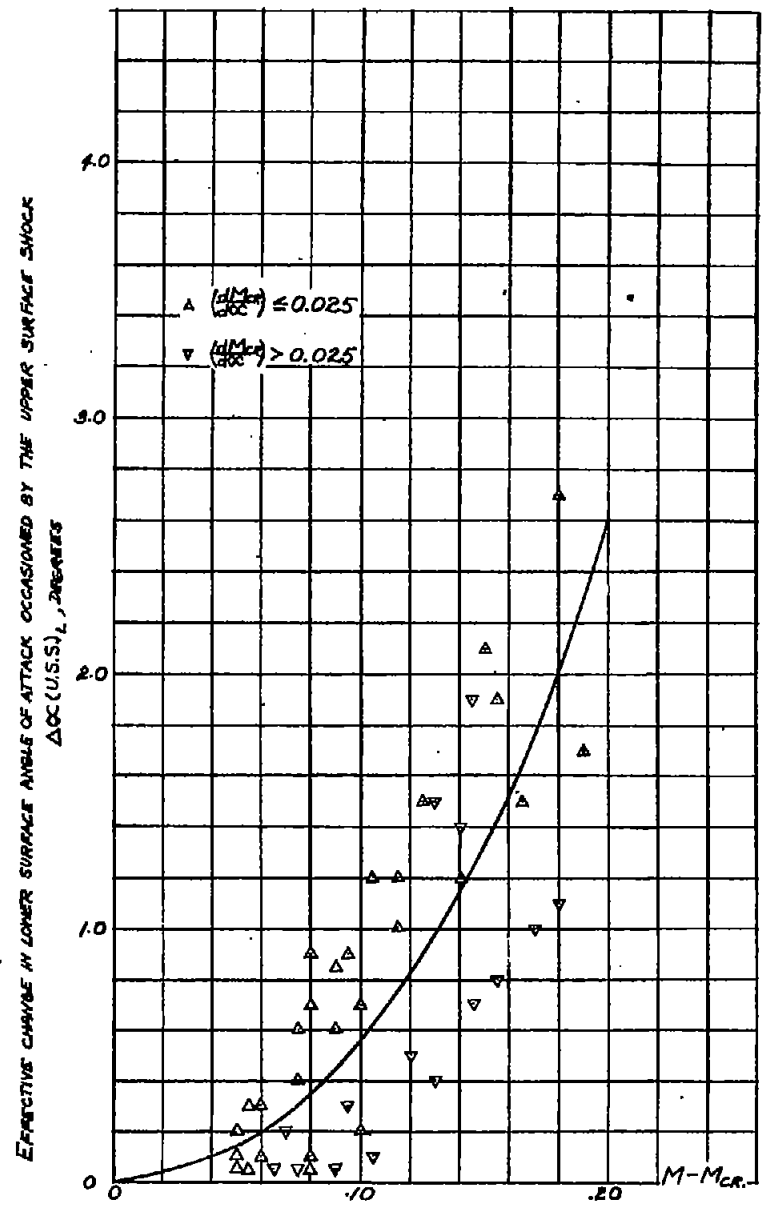


FIGURE 2.- EFFECTIVE CHANGE IN LOWER SURFACE ANGLE OF ATTACK WITH INCREMENT OF MACH NUMBER ABOVE THE CRITICAL.

NAACA RM. NO. 47307

CONFIDENTIAL

FIG. 1,2

CONFIDENTIAL

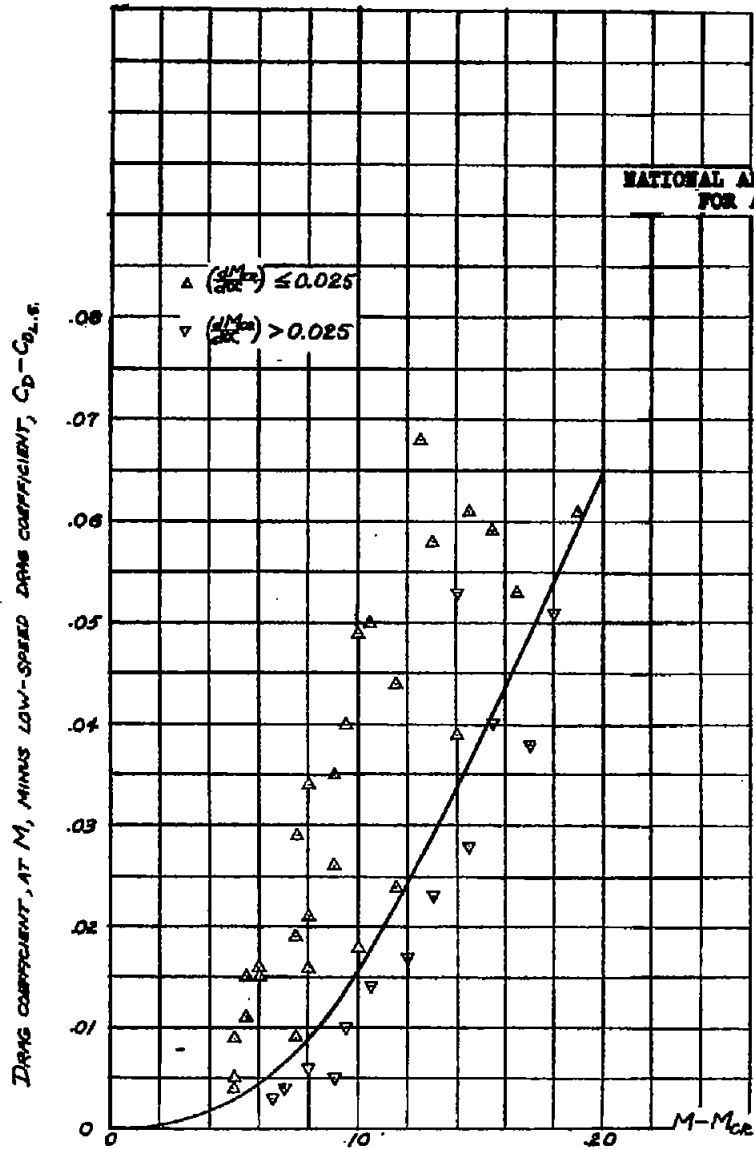


FIGURE 3.- DRAG COEFFICIENT INCREASE FOR MACH NUMBER INCREMENTS ABOVE THE CRITICAL AT MODERATE ANGLES OF ATTACK.

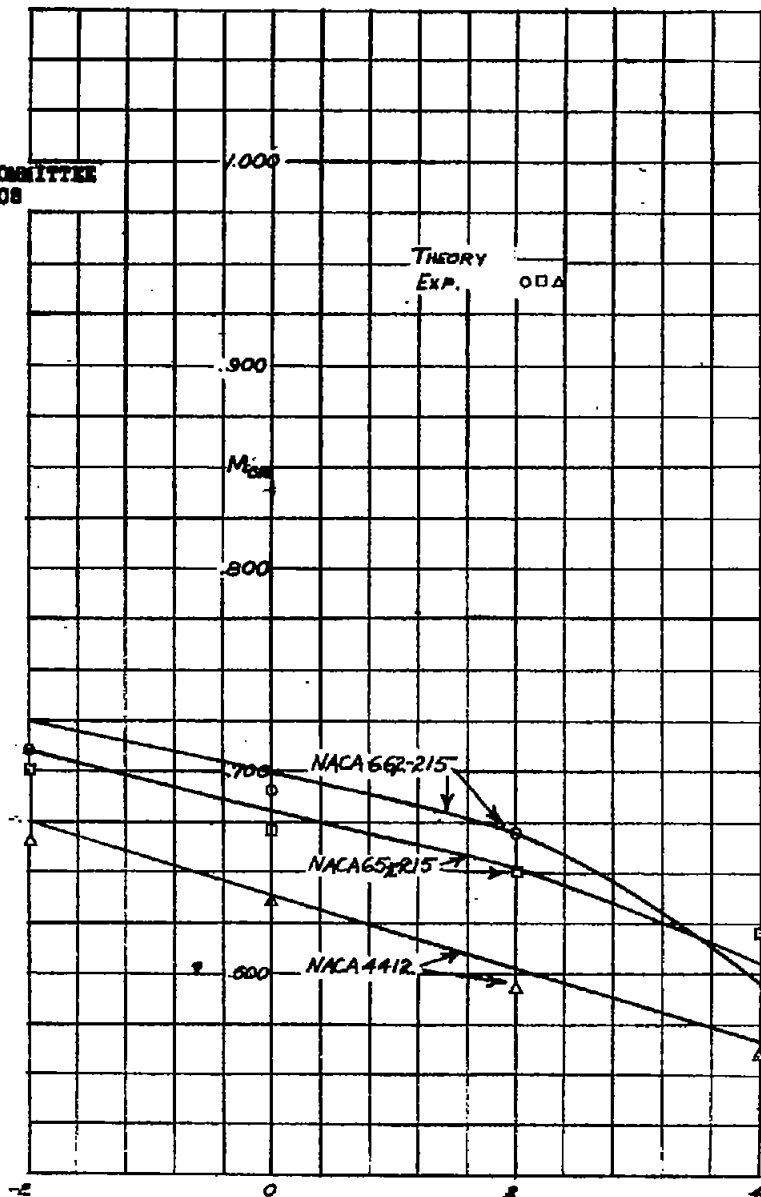


FIGURE 4.- VARIATION OF CRITICAL MACH NUMBER WITH ANGLE OF ATTACK, (a) UPPER SURFACE: NACA 652-215, 662-215 AND 4412 AIRFOILS.

FIG. 3, 4a

CONFIDENTIAL

NACA RM No. A7807

CONFIDENTIAL

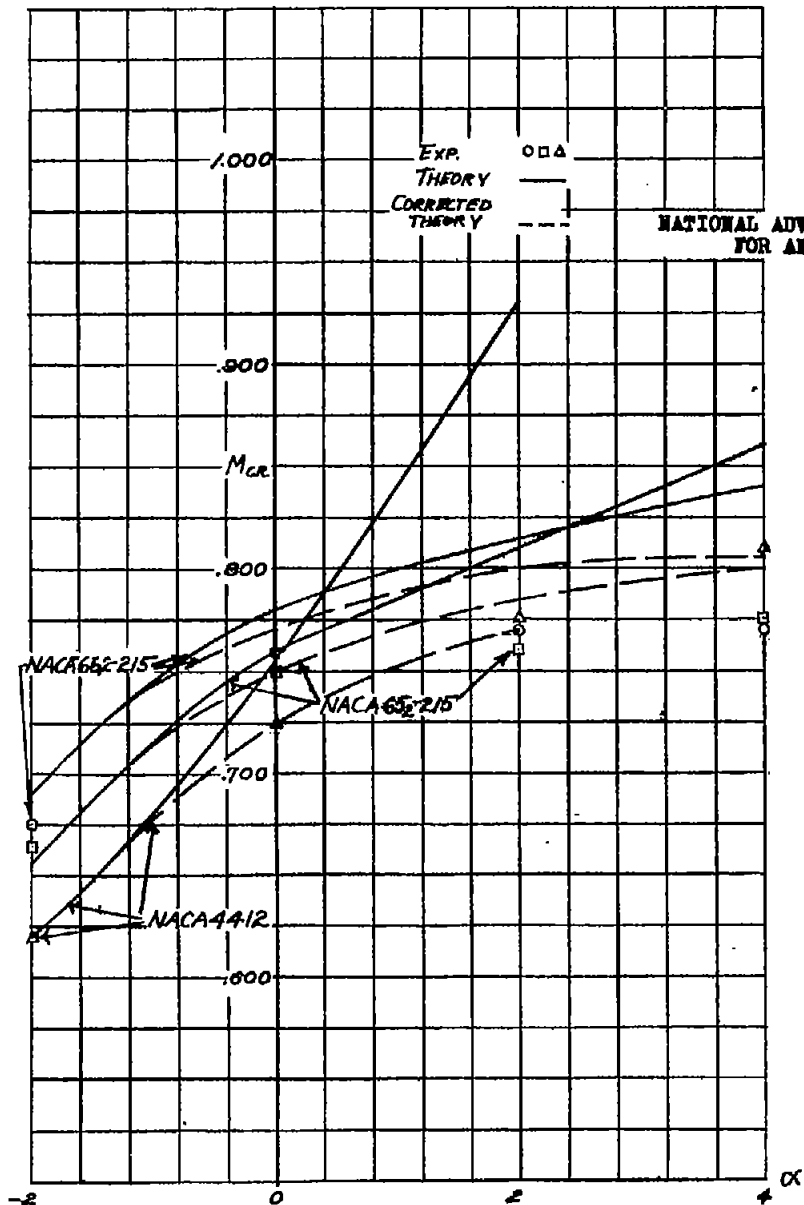


FIGURE 4.- (CONTINUED), CRITICAL MACH NUMBER
 (b) LOWER SURFACE: NACA 65-215, 66-215 AND 4412 AIRFOILS

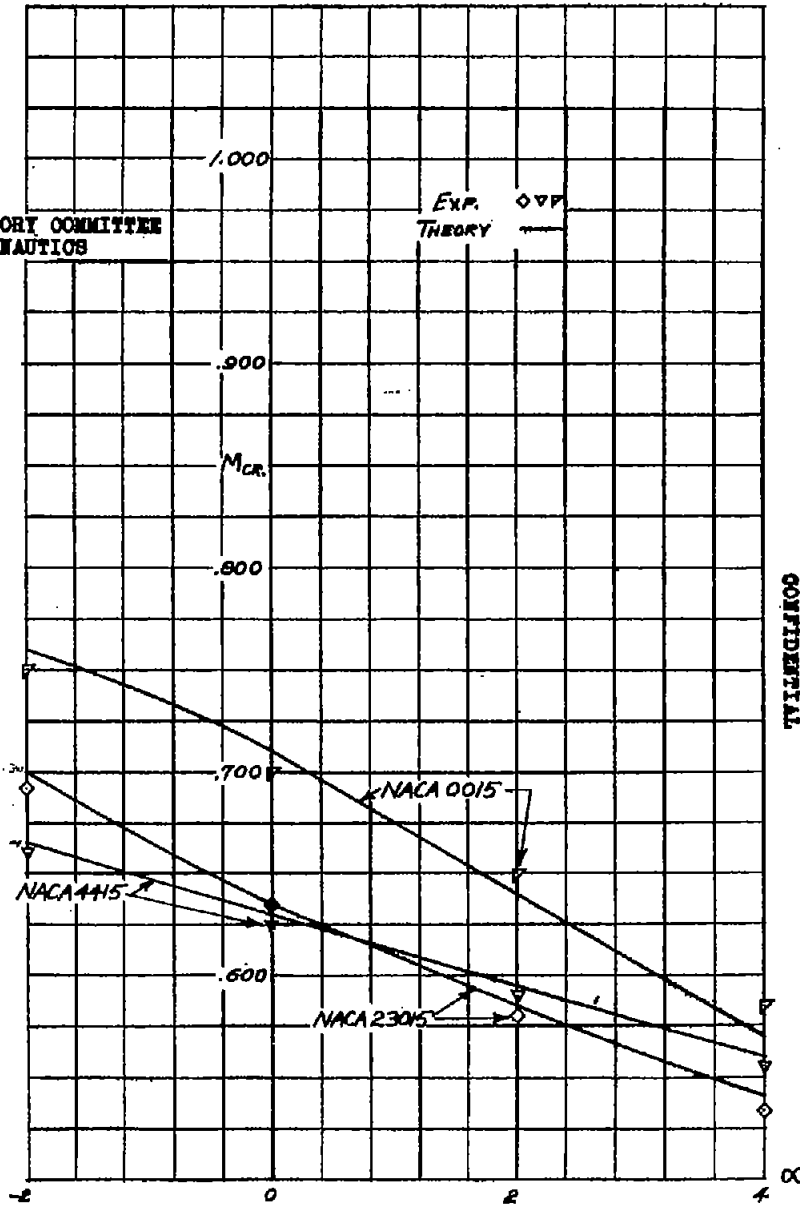


FIGURE 4.- (CONTINUED), CRITICAL MACH NUMBER
 (c) UPPER SURFACE: NACA 0015, 23015, AND 4415 AIRFOILS

NACA RM. No. A7807

CONFIDENTIAL

FIG. 4b,c

Figs. 4d,5

NACA RM No. A7B07

CONFIDENTIAL

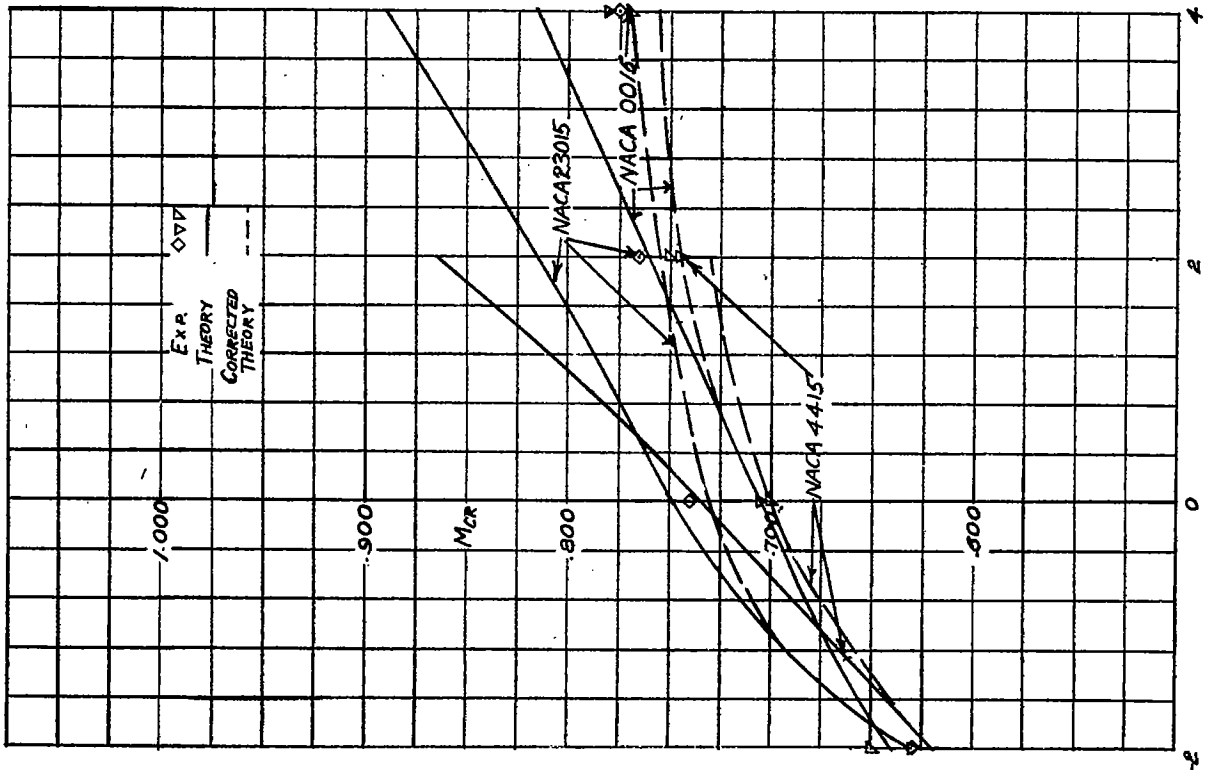


FIGURE 4.- (CONCLUDED) CRITICAL MACH NUMBER
 (d) LOWER SURFACE: NACA 0015, 23015, AND 4415 AIRFOILS

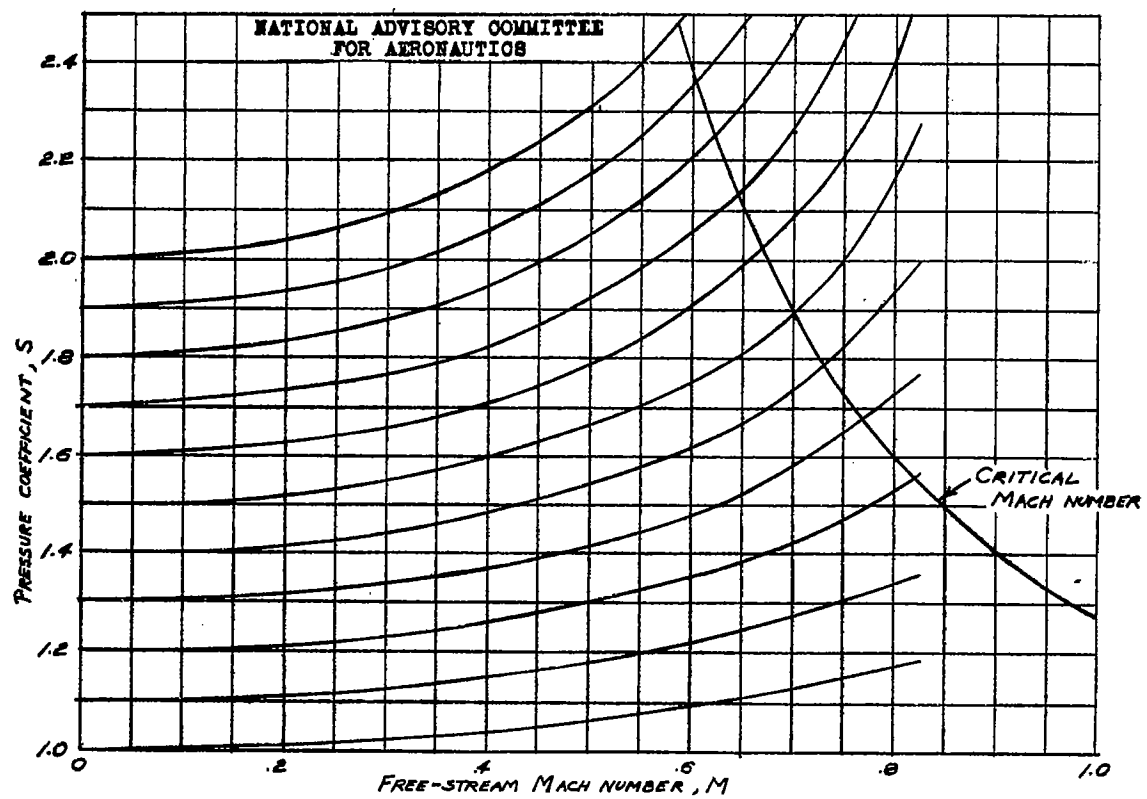


FIGURE 5.- KÁRMÁN-TSIEN THEORETICAL COMPRESSIBILITY CORRECTION FOR PRESSURE COEFFICIENTS.
 CONFIDENTIAL

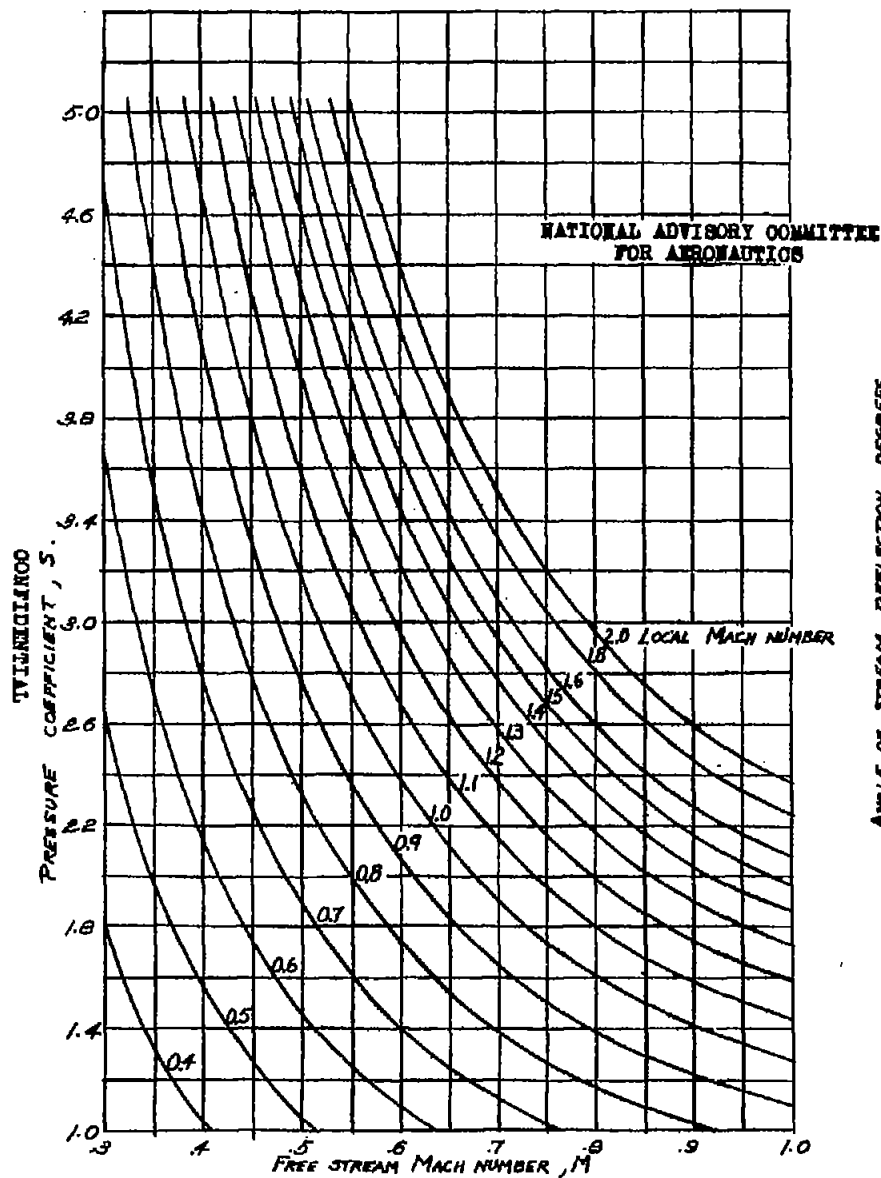


FIGURE 6.- VARIATION OF LOCAL MACH NUMBER WITH PRESSURE COEFFICIENT AND FREE-STREAM MACH NUMBER.

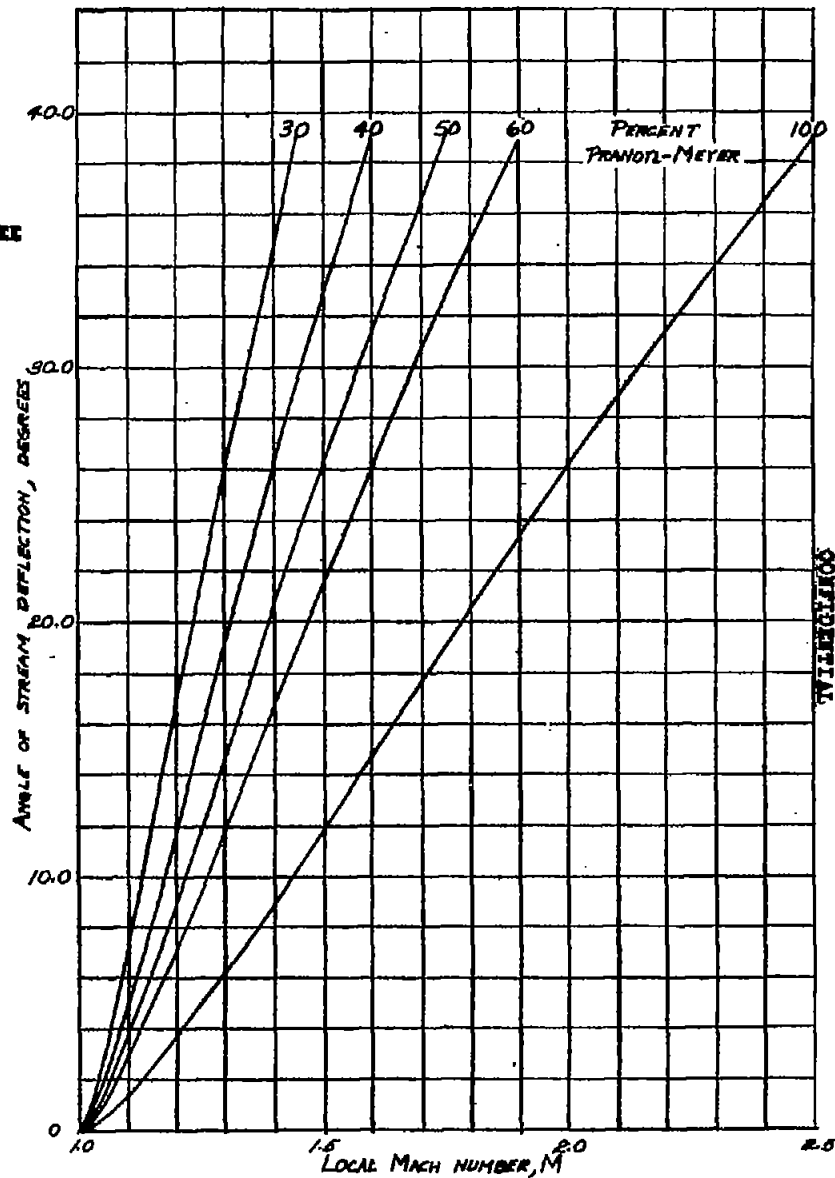


FIGURE 7.- PERCENTAGES OF PRANDTL-MEYER THEORETICAL VARIATION OF LOCAL MACH NUMBER WITH ANGLE OF STREAM DEFLECTION.

KNOW RM NO. A7507

CONFIDENTIAL

FIGS. 6, 7

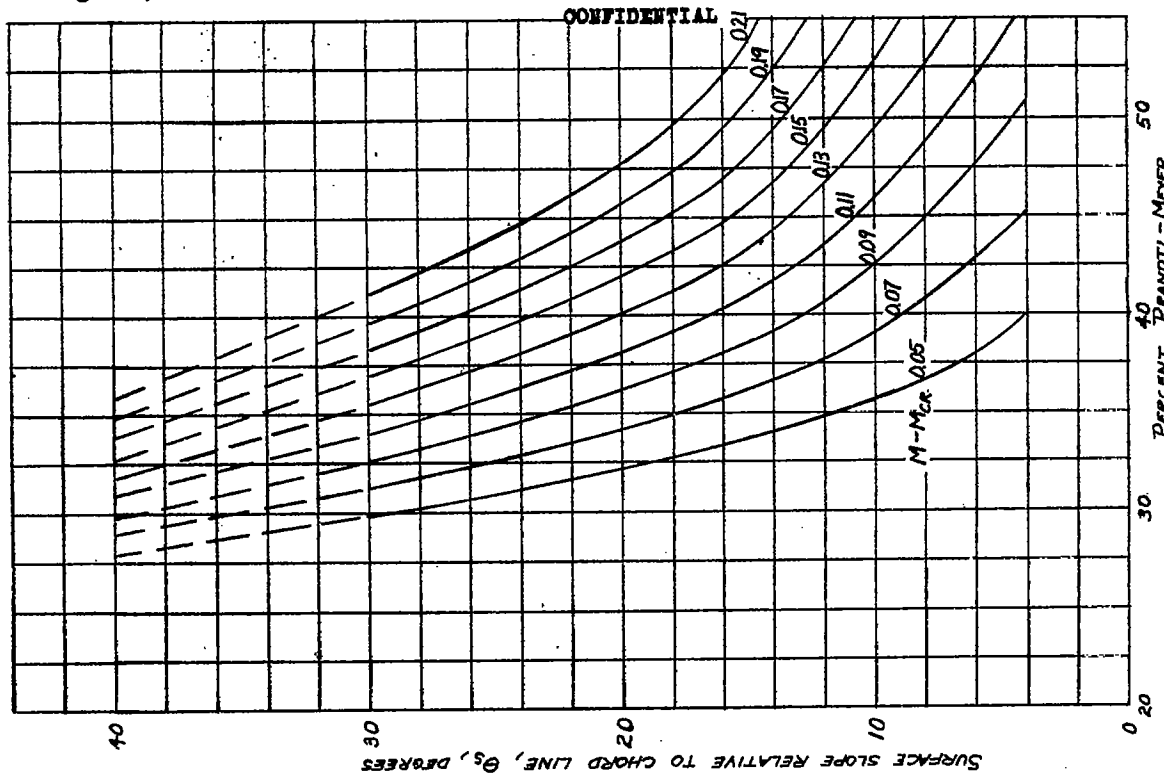


FIGURE 8.- PERCENT OF PRANDTL-MEYER THEORY ATTAINED FOR VARIOUS VALUES OF $M-M_{CR}$ AS A FUNCTION OF THE AIRFOIL SURFACE SLOPE AT SONIC POINT.

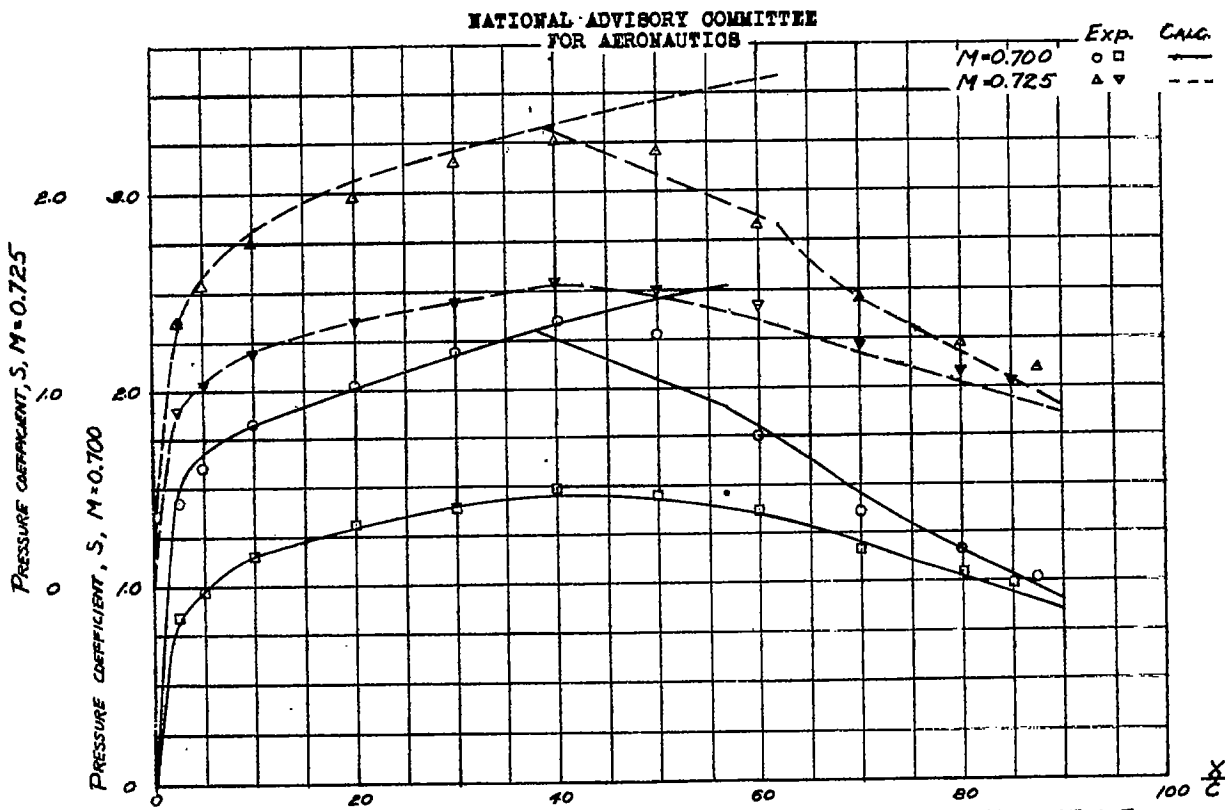


FIGURE 9.- CALCULATED AND EXPERIMENTAL PRESSURE DISTRIBUTIONS FOR NACA 65E215 AIRFOIL
 (a) $\alpha=2^\circ$ $M=0.700$ AND 0.725

NACA RM No. A7B07

Figs. 9b,c

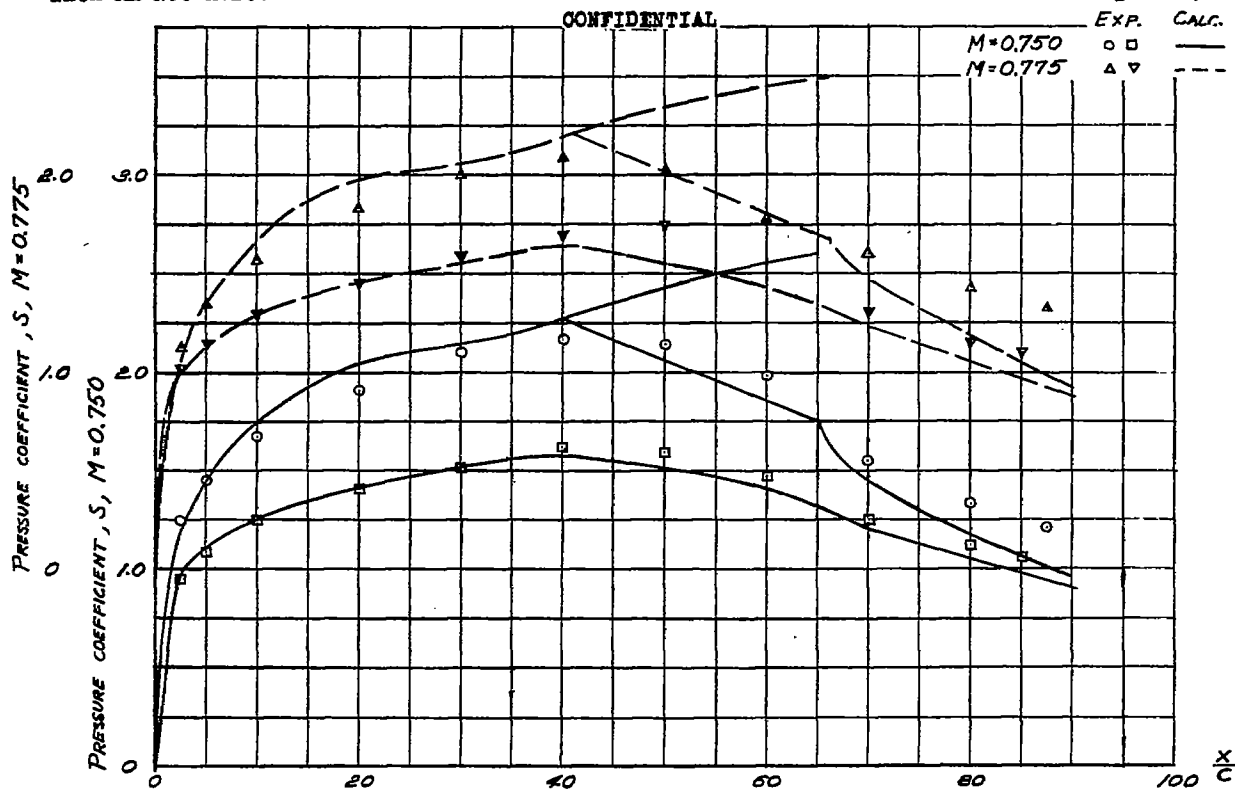


FIGURE 9.—(CONTINUED), NACA 65-215 AIRFOIL.
 (b) $\alpha = 2^\circ$; $M = 0.750$ AND 0.775

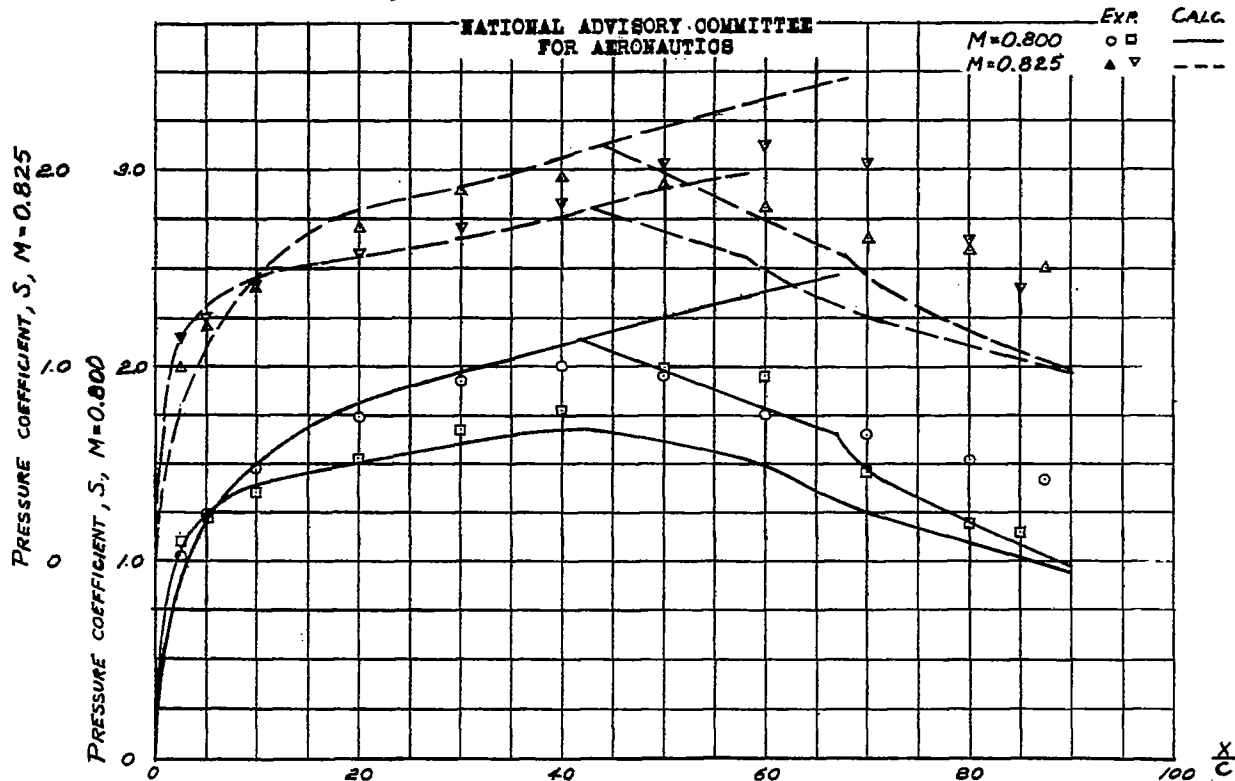


FIGURE 9.—(CONTINUED), NACA 65-215 AIRFOIL.
 (c) $\alpha = 2^\circ$; $M = 0.800$ AND 0.825 .

CONFIDENTIAL

Figs. 9d, e

NACA RM No. A7B07

CONFIDENTIAL

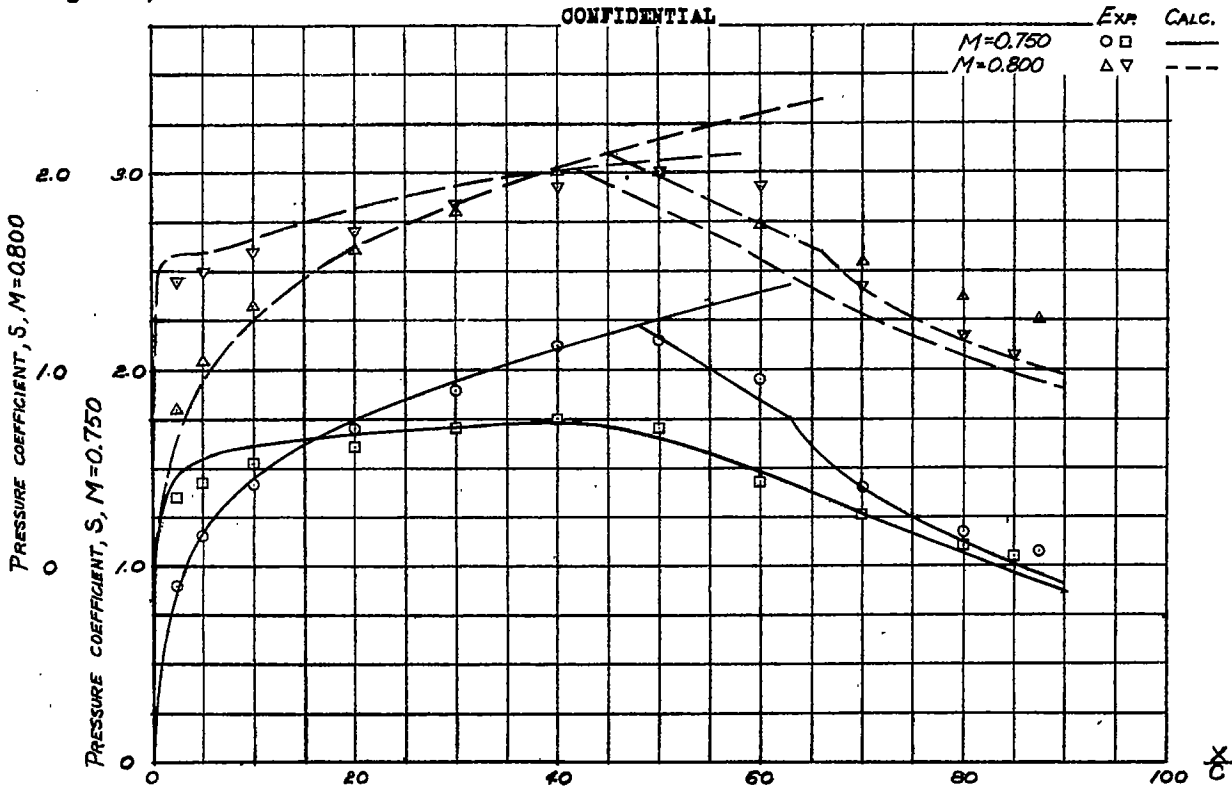


FIGURE 9.- (CONTINUED) NACA 65₂-215 AIRFOIL
 (d) $\alpha=0^\circ$ M=0.750 AND 0.800

NATIONAL ADVISORY COMMITTEE
 FOR AERONAUTICS

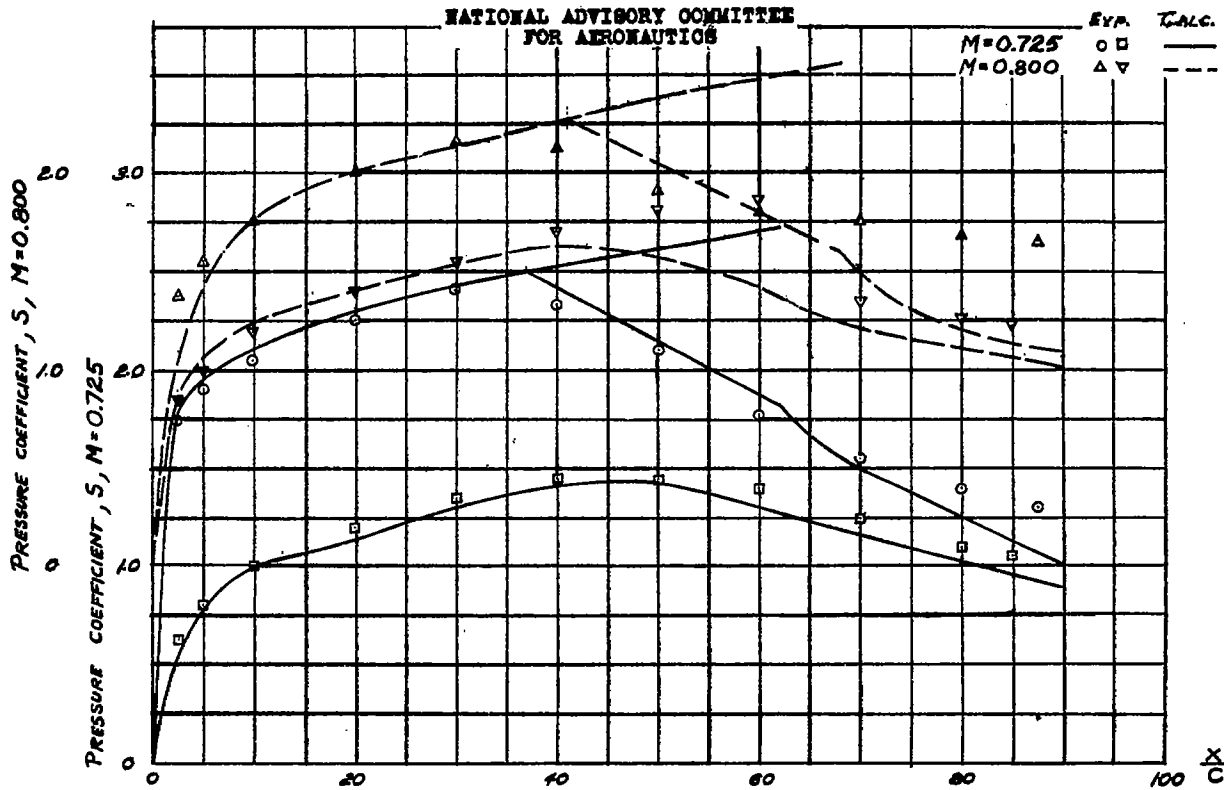


FIGURE 9.- (CONCLUDED) NACA 65₂-215 AIRFOIL
 (e) $\alpha=4^\circ$, M=0.725 AND 0.800.

CONFIDENTIAL

NACA RM No. A7B07

Figs. 10a,b

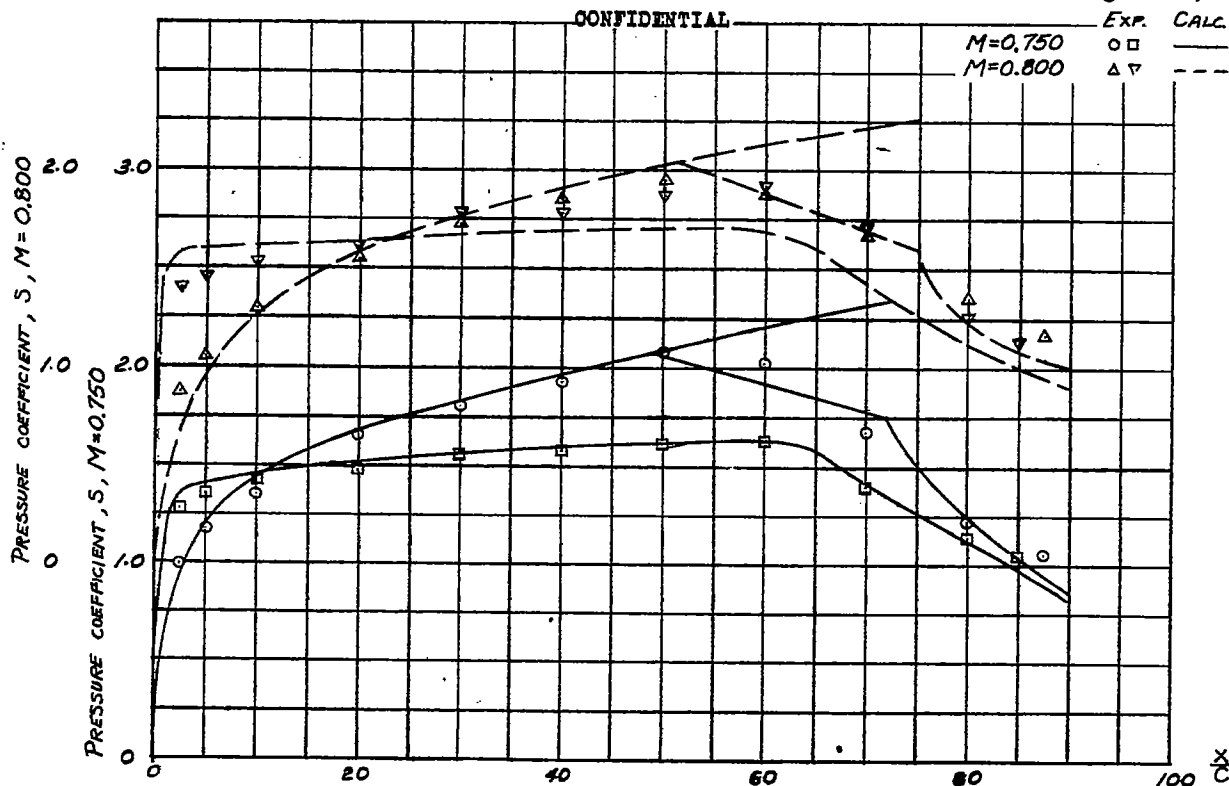


FIGURE 10.-CALCULATED AND EXPERIMENTAL PRESSURE DISTRIBUTIONS FOR NACA 66,2-215 AIRFOIL.
 (a) $\alpha = 0^\circ$; $M = 0.750$ AND 0.800

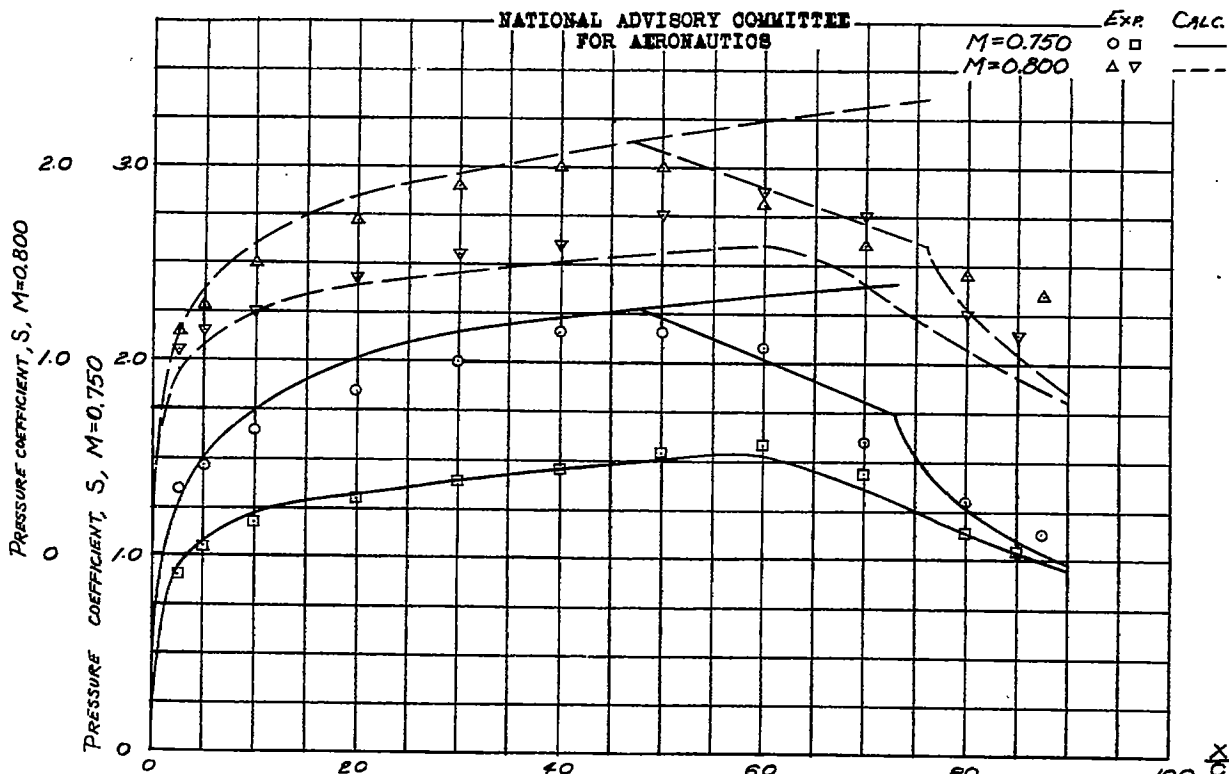


FIGURE 10.- (CONTINUED) , NACA 66,2-215 AIRFOIL.
 (b) $\alpha = 2^\circ$; $M = 0.750$ AND 0.800

CONFIDENTIAL

Figs. 10c, 11a

NACA RM No. A7B07

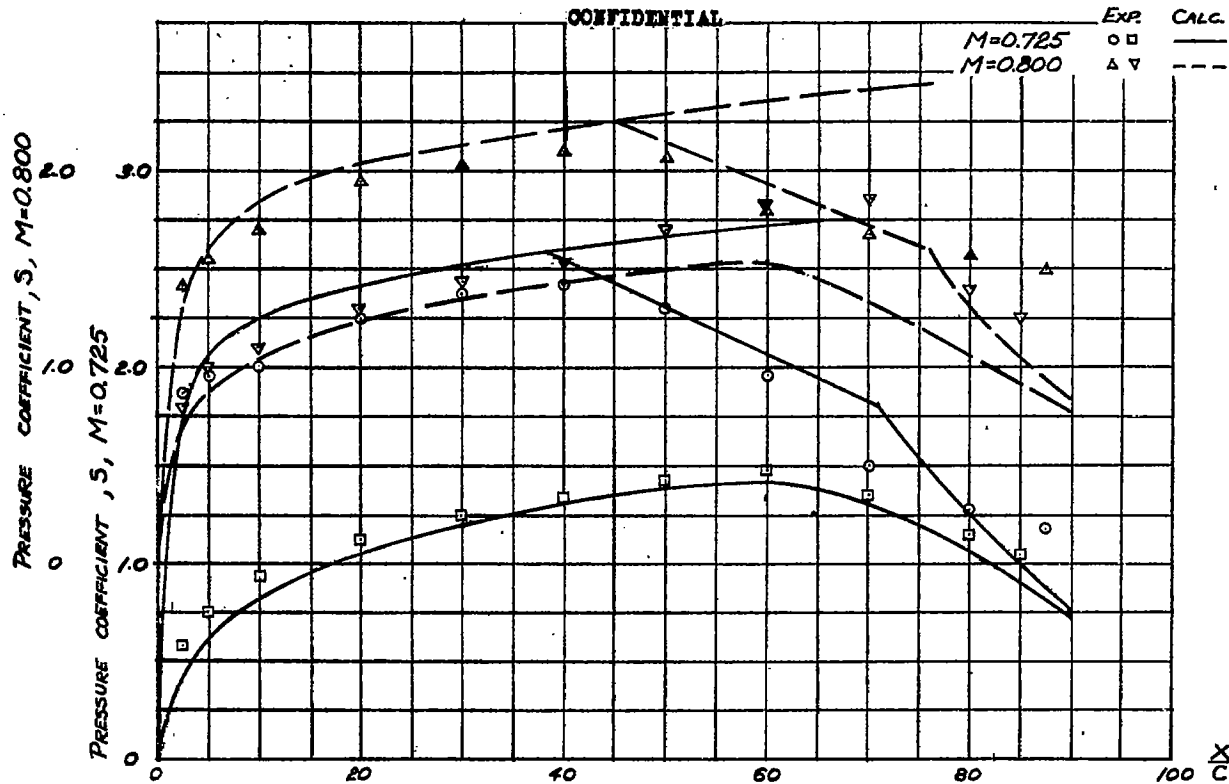


FIGURE 10.- (CONCLUDED) NACA 66,2-215 AIRFOIL
 (c) $\alpha = 4^\circ$; $M = 0.725$ AND 0.800

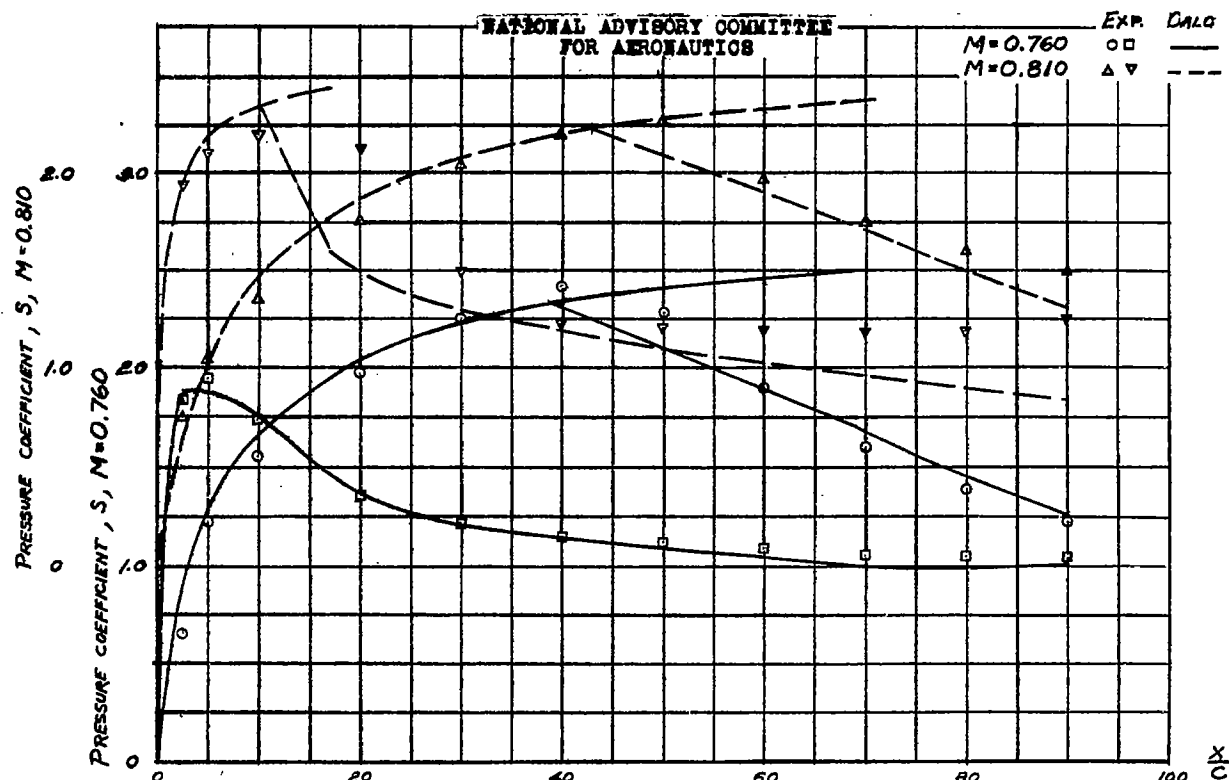
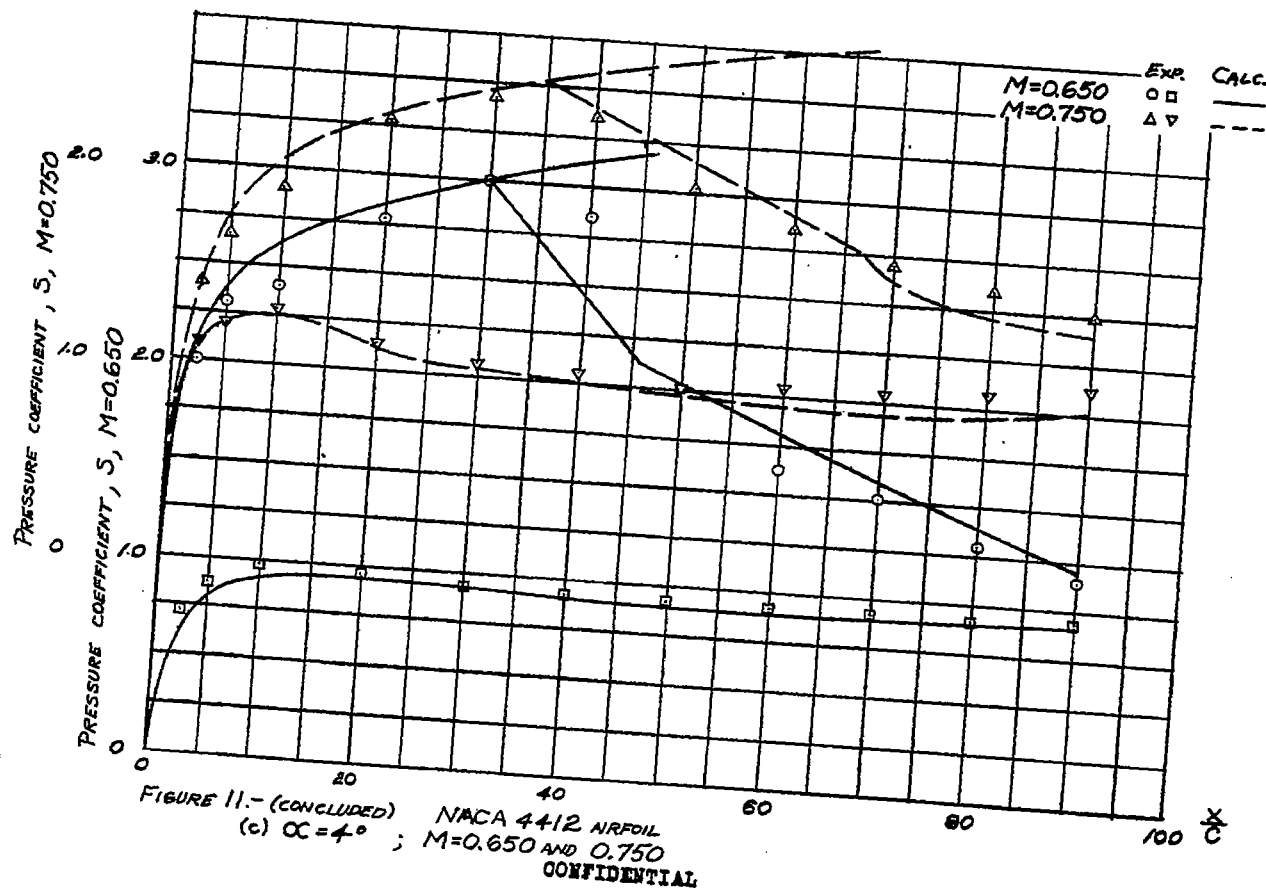
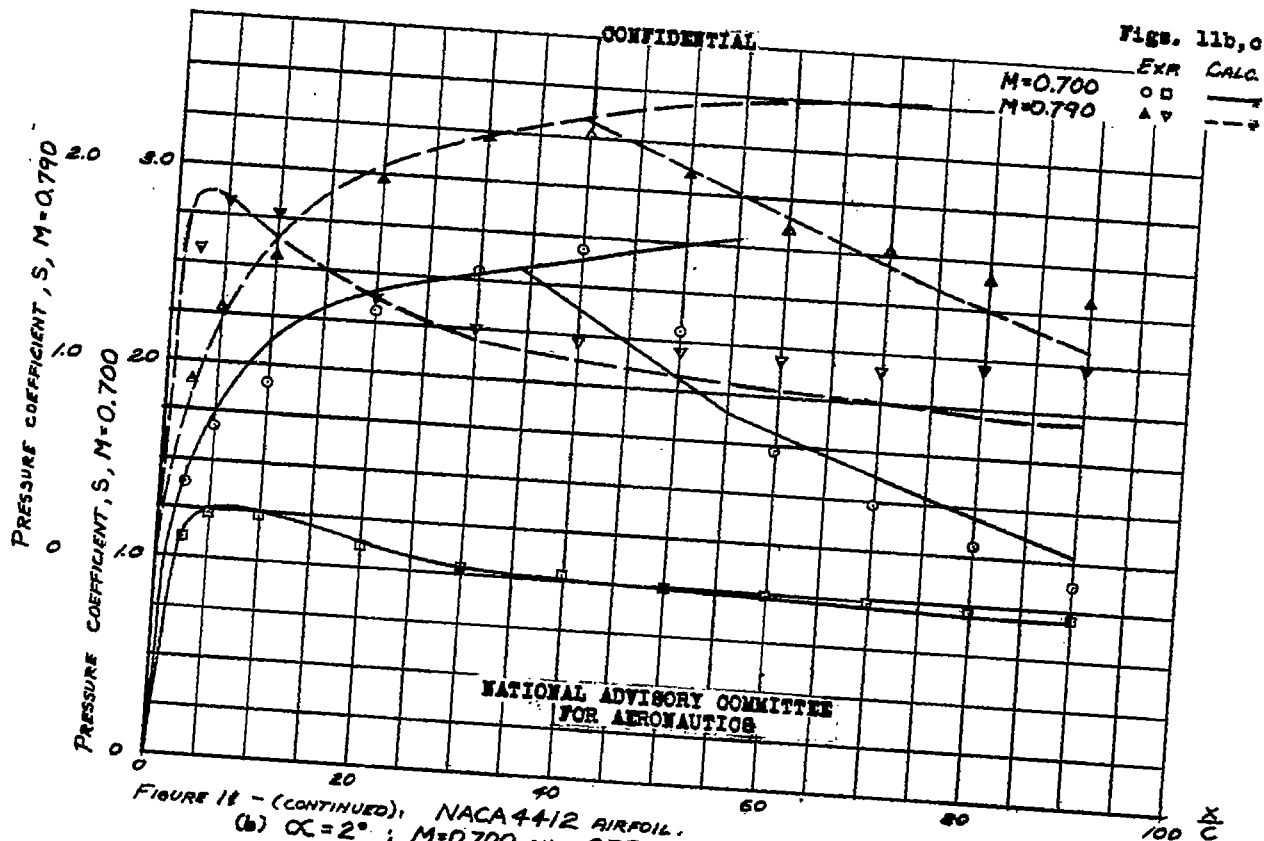


FIGURE 11.- CALCULATED AND EXPERIMENTAL PRESSURE DISTRIBUTIONS FOR NACA 4412 AIRFOIL
 (a) $\alpha = 0^\circ$; $M = 0.760$ AND 0.810

CONFIDENTIAL

NACA RM No. A7B07



Figs. 12a,b

NACA RM No. A7B07

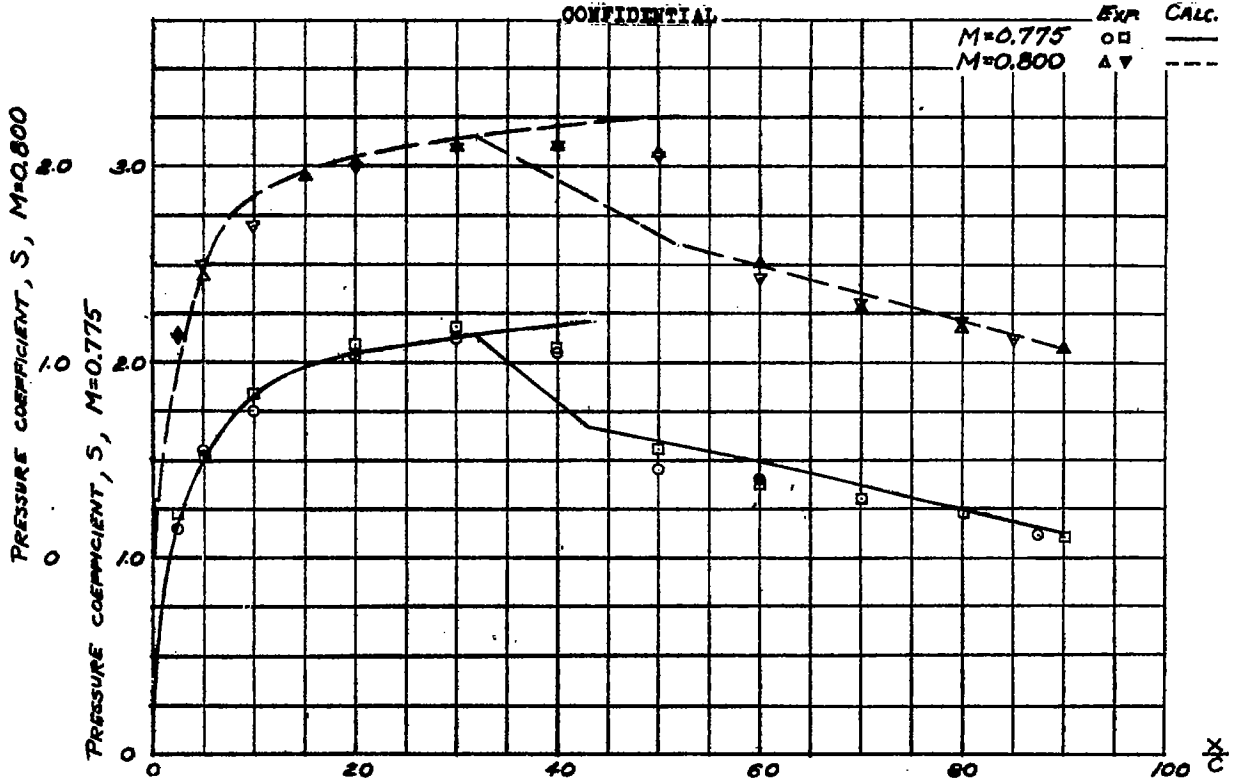


FIGURE 12.- CALCULATED AND EXPERIMENTAL PRESSURE DISTRIBUTIONS FOR NACA 0015 AIRFOIL
 (a) $\alpha = 0^\circ$; $M = 0.775$ AND 0.800

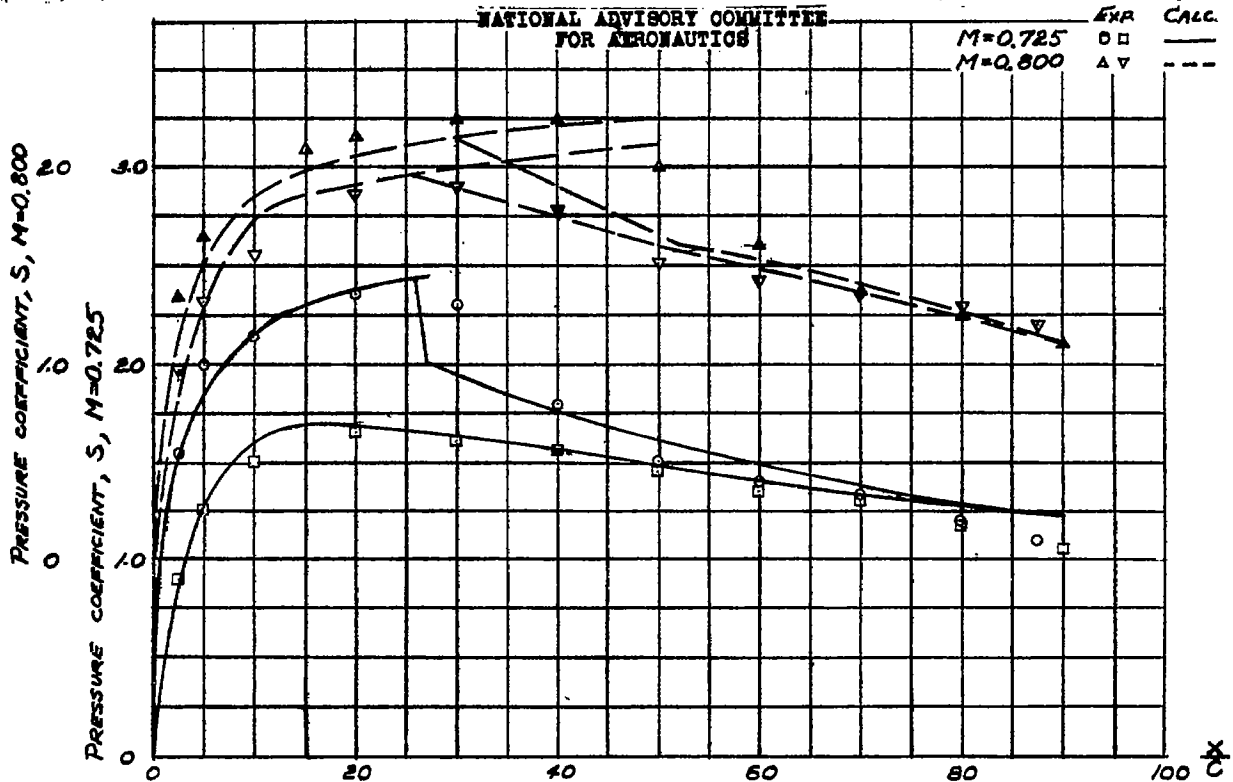


FIGURE 12.- (CONTINUED) NACA 0015 AIRFOIL
 (b) $\alpha = 2^\circ$; $M = 0.785$ AND 0.800

CONFIDENTIAL

CONFIDENTIAL

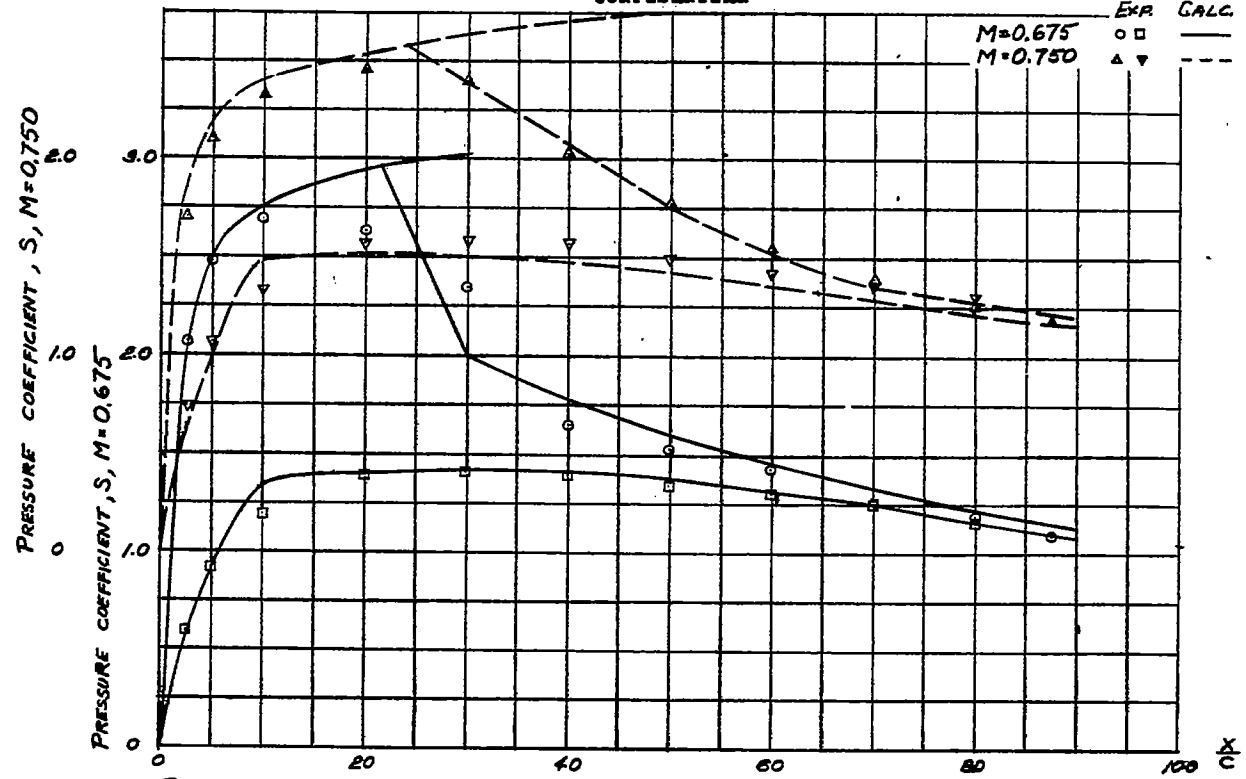


FIGURE 12.- (CONCLUDED) NACA 0015 AIRFOIL.
 (c) $\alpha = 4^\circ$; $M = 0.675$ AND 0.750

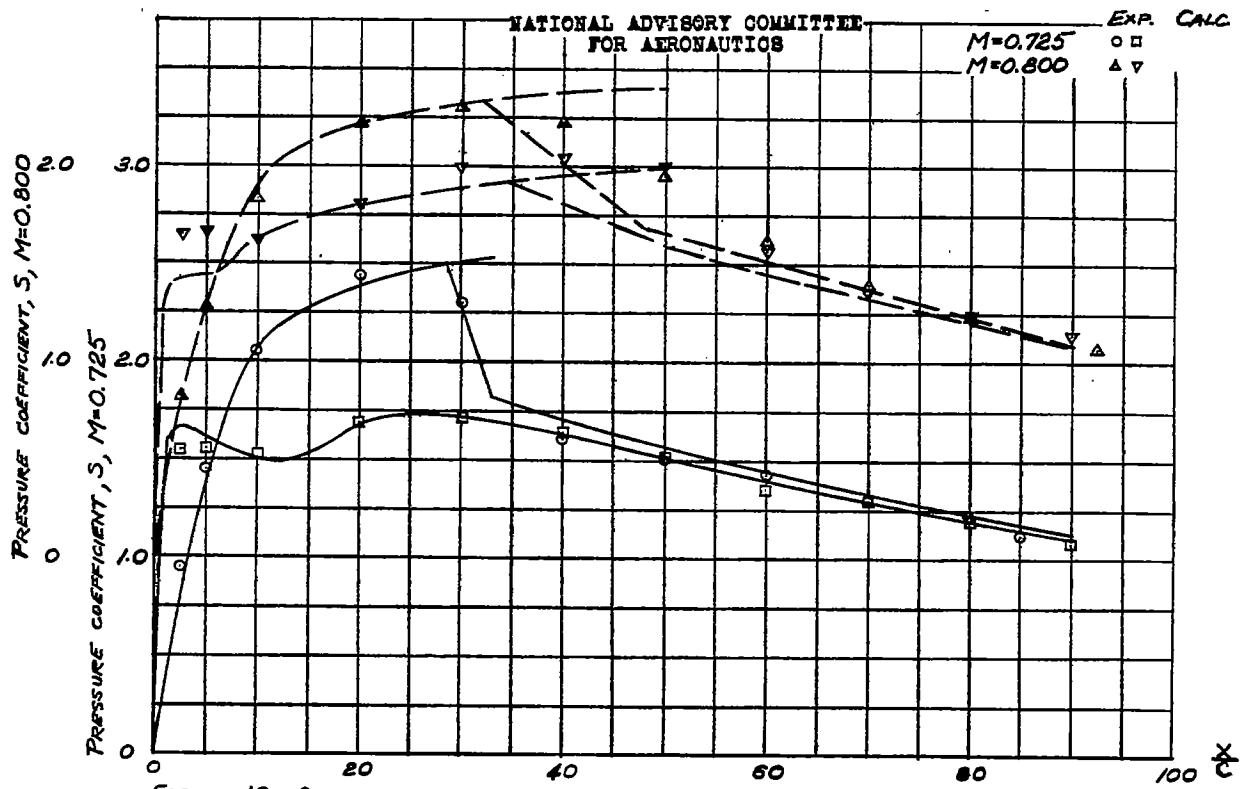


FIGURE 13.- CALCULATED AND EXPERIMENTAL PRESSURE DISTRIBUTIONS FOR NACA 23015 AIRFOIL
 (a) $\alpha = 0^\circ$; $M = 0.725$ AND 0.800

CONFIDENTIAL

Figs, 13b,c

NACA RM No. A7807

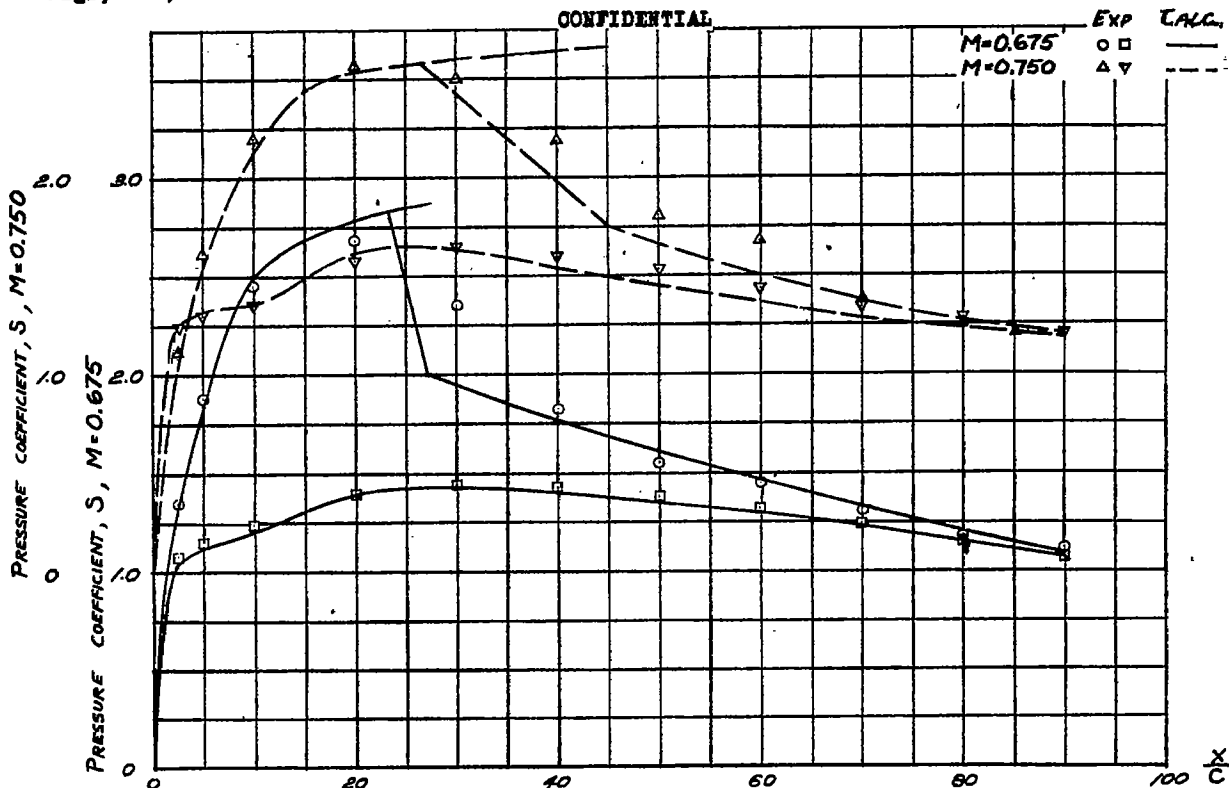


FIGURE 13.- (CONTINUED) NACA 23015 AIRFOIL
 (b) $\alpha = 2^\circ$; $M=0.675$ AND 0.750

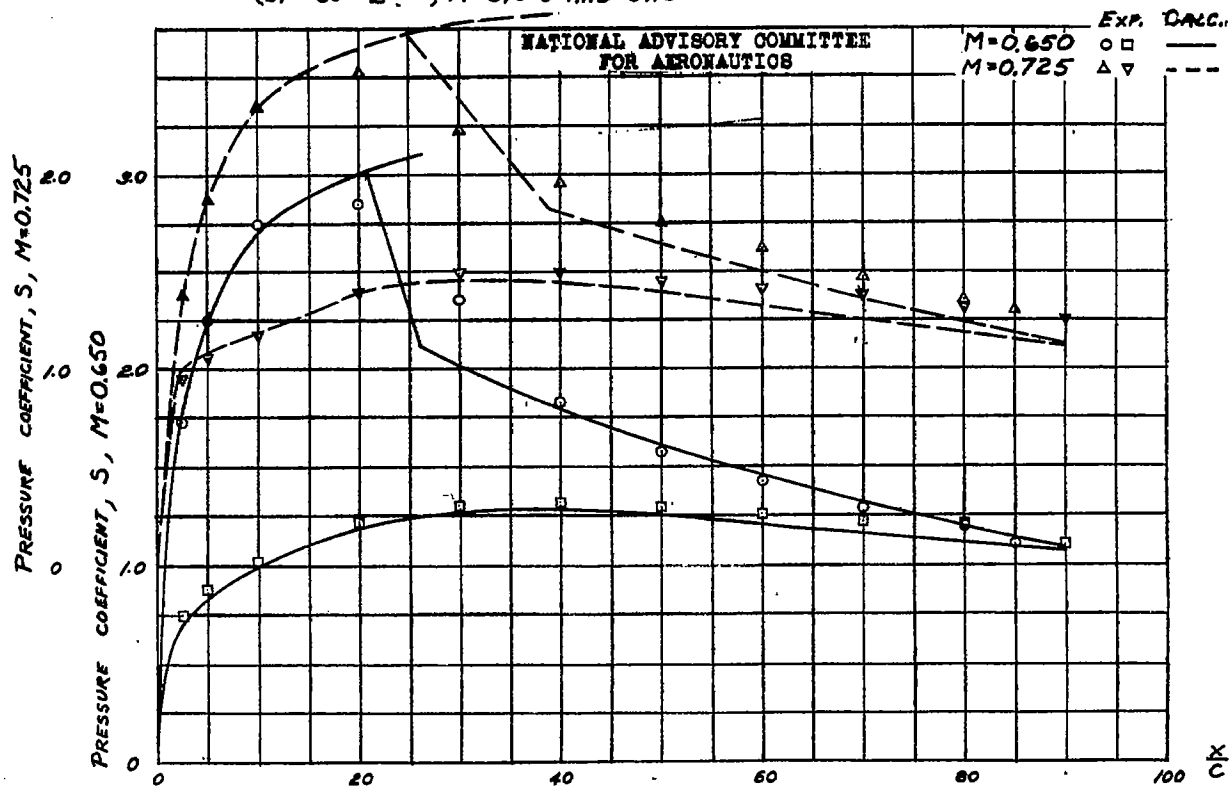


FIGURE 13.- (CONCLUDED) NACA 23015 AIRFOIL
 (c) $\alpha = 4^\circ$; $M=0.650$ AND 0.725

CONFIDENTIAL

NACA RM No. A7B07

Fig. 14a,b

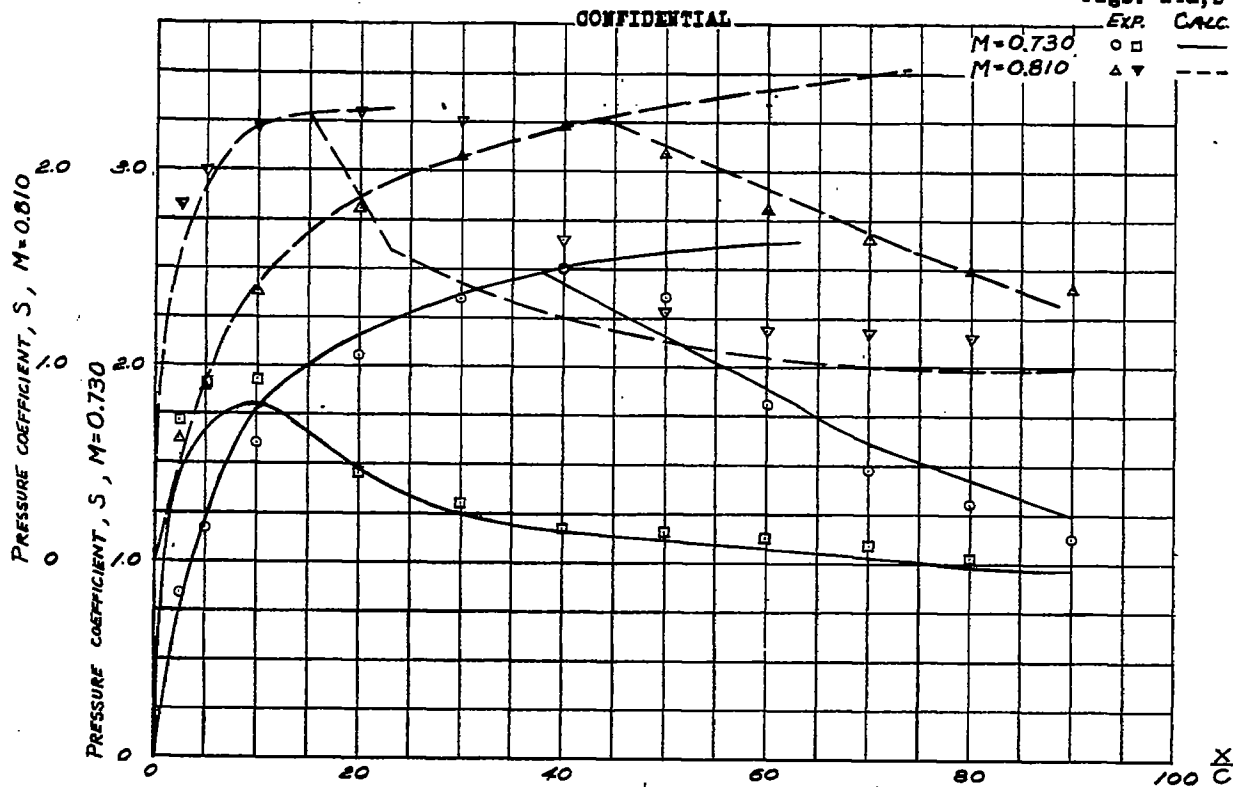


FIGURE 14.- CALCULATED AND EXPERIMENTAL PRESSURE DISTRIBUTIONS FOR NACA 4415 AIRFOIL
 (a) $\alpha = 0^\circ$; $M = 0.730$ AND 0.810
 NATIONAL ADVISORY COMMITTEE
 FOR AERONAUTICS

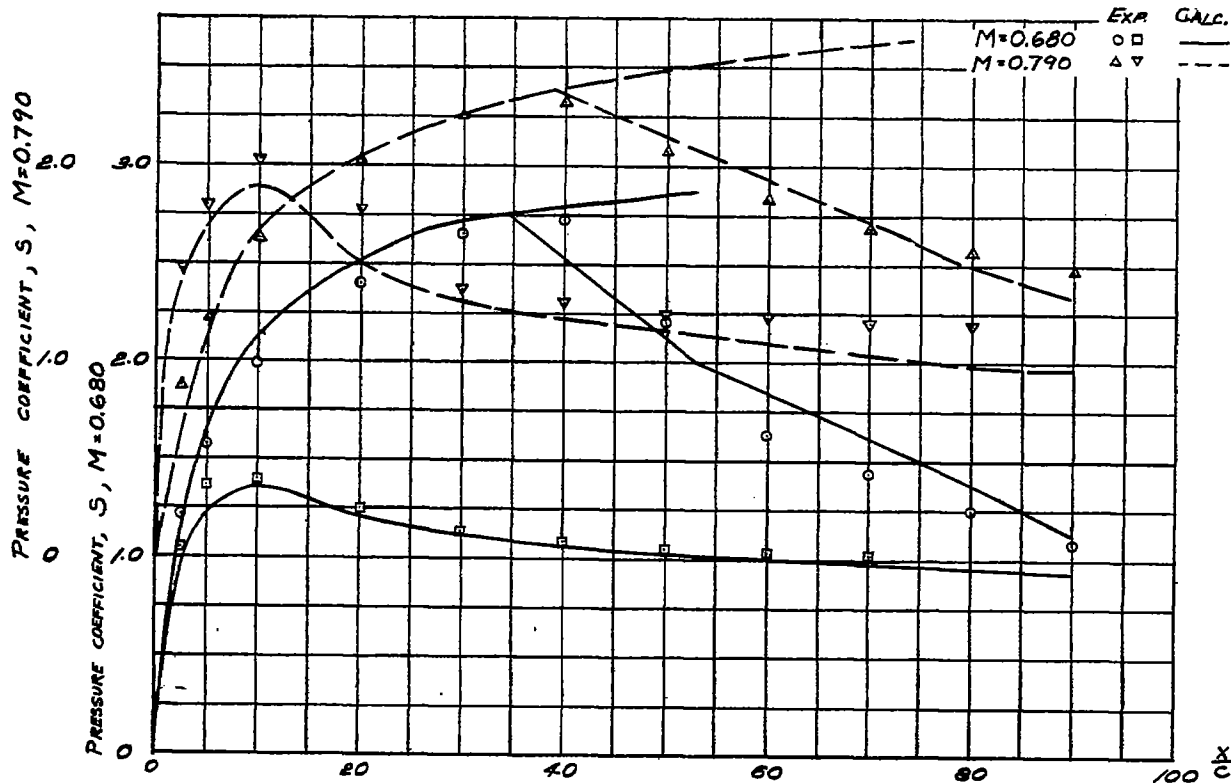
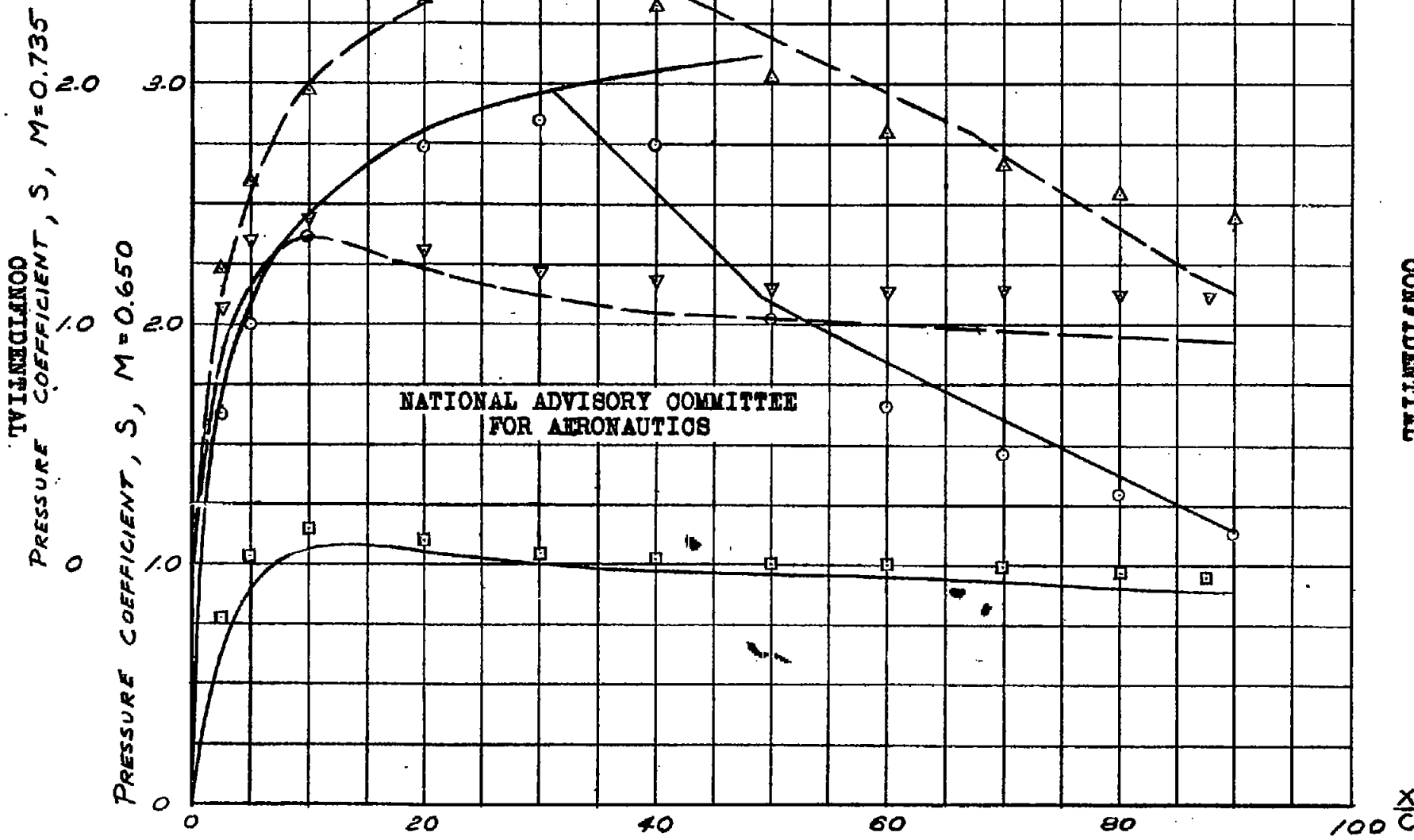


FIGURE 14.- (CONTINUED) NACA 4415 AIRFOIL
 (b) $\alpha = 2^\circ$; $M = 0.680$ AND 0.790
CONFIDENTIAL

CONFIDENTIAL



NATIONAL ADVISORY COMMITTEE
 FOR AERONAUTICS

FIGURE 14.- (CONCLUDED) NACA 4415 AIRFOIL
 (c) $\alpha = 4^\circ$; $M = 0.650$ AND 0.735

CONFIDENTIAL

FIG. 14c

NACA RM No. A7807

X/C